5-12-2022

Assessing red spruce (Picea rubens) restoration potential under current and future predicted climate change in Virginia

Christian Brown

Assessing red spruce (*Picea rubens*) restoration potential under current and future predicted climate change in Virginia

Christian Brown

A thesis submitted to the Graduate Faculty of

JAMES MADISON UNIVERSITY

In

Partial Fulfillment of the Requirements

for the degree of

Master of Science

Department of Biology

May 2022

FACULTY COMMITTEE:

Committee Chair: Dr. Heather P. Griscom

Committee Members/ Readers:

Dr. Patrice Ludwig

Dr. Bruce Wiggins

Table of Contents

LIST OF TABLES

LIST OF FIGURES

ABSTRACT

Global climate change threatens many species across the planet. High-elevation species, such as red spruce (*Picea rubens*), face significant and immediate threats from climate change. Red spruce has faced anthropogenic disturbances for over a century and is only recently beginning to regenerate across its range, making it an ideal restoration candidate. Ecological niche modeling has become a common method of identifying the suitable habitat of a species, providing vital information to land managers carrying out restoration efforts. In this study ecological niche models were used in a novel way, predicting distribution and habitat suitability separately to determine the spatial extent to which red spruce can be restored. In addition to models, surveys were conducted to elucidate the current regeneration trends of red spruce. Furthermore, climate projections were used to determine how restoration potential may change over the course of the 21st century. Comparisons between distribution and habitat suitability models indicate that there is additional habitat available for red spruce to expand into. Regeneration surveys show that there is positive regeneration both within and beyond red spruce canopies, validating model comparisons. Climate change projections indicate total elimination of suitable habitat in Virginia by 2100. However, these projections likely predict increased competition for red spruce from low elevation competitors as opposed to physiological limitations imposed by climate change. It is therefore prudent to protect established populations and encourage further regeneration by planting in higher elevations where competition is more limited.

INTRODUCTION

Ecological niche models (ENMs) are powerful computational tools used to understand current and potential species distributions, test biogeographic hypotheses, and forecast anthropogenic impacts on species. ENMs relate observations of species occurrence and absence to their environment in order to then approximate some aspect of the distribution of that species across space and time (Guisan et al. 2017, Guisan and Thuiller 2005). Such models provide practical information which can inform conservation and restoration management practices, often in the form of map projections of habitat suitability or species distributions. The terms in the field of ecological niche modeling, such as ecological niche model, species distribution model (SDM), and habitat suitability model (HSM) are often used interchangeably, although each term can have very different meanings depending on the context of the study. The appropriate usage of modeling terminology has even been the subject of a review, though the literature still conflates different terms with each other (Peterson and Soberon 2012). For the purposes of this study ENM was used as an umbrella term to describe both SDMs and HSMs. Further, SDM was used to describe models which aim to predict the current distribution of a species, whereas HSM was used to describe models which aim to predict the potential distribution of a species given its suitable habitat.

ENMs are broadly applicable across species of both rare and ample abundance in marine, aquatic, and terrestrial environments (Williams-Tripp et al. 2012, Kaschner et al. 2006, Ahmadi-Nedushan et al. 2006, Leblond et al. 2014). Of particular contemporary relevance is the time projection capability of ENMs through the alteration of environmental variable data. Climate change is expected to have a significant effect on

the range of many species, with many range shifts already underway (Parmesan and Yohe 2003). ENMs are able to forecast the effects of various climate change scenarios on the distribution of a species (Thuiller 2004). For example, ENMs were used to forecast the range of *Pinus pumila*, a dominant alpine tree species in Japan. Models indicated that *P. pumila* will lose 14.7% of its suitable habitat by 2100 in mild climate change scenarios and up to 25% of its suitable habitat in severe climate change scenarios (Horikawa et al. 2009). Predicting how a species' range will be affected by climate change allows land managers to make strategic and well-informed conservation and restoration decisions, with the potential to conserve many ecosystems. Forests are important biodiverse ecosystems and therefore are often the subject of ENMs which aim to project major ecological consequences of climate change.

Mountain forests are ecologically and economically valuable habitats that provide an abundance of ecosystem services. Mountains constitute 24% of all land on Earth. Excluding Antarctica, forests cover 1/3 of all mountainous terrain and comprise 9 million km^2 or 28% of total closed forest area on the planet (Kapos et al. 2000). Forests also serve as carbon sinks, estimated to absorb 2.4 petagrams of carbon annually (Pan et al. 2011). Among the most valuable ecosystem services offered by mountains is watershed regulation and protection. Many watersheds originate in the mountains, which provide anywhere from 30%-95% of downstream water flow in various regions of the world. This downstream flow provides fresh water for drinking, irrigation, transportation, fishing and recreation (Price 2003). High elevation forests also protect the quality of watersheds by reducing erosion and stream sedimentation (Liniger and Weingartner 2000). Mountain forests are biodiversity hotspots, often supporting more biodiversity than lowland forests

(Price 2003). These vital ecosystems face numerous challenges of anthropogenic origin including habitat fragmentation, deforestation, and climate change.

The tree species that comprise high elevation forests are extremely vulnerable to climate change. With increasing temperatures, the suitable habitat available to high elevation tree species is expected to diminish and retreat upwards in elevation (Potter et al. 2010). In the Swiss Alps, the tree line was found to have already slightly shifted upwards in elevation due in part to climate change (Gehrig-Fasel et al. 2007). Concurrently, low elevation plant species are predicted to migrate upwards in elevation, thus burdening high elevation trees with increased competition (Bell et al. 2014). Further exacerbating the threat of climate change is the island-like distribution of many tree species endemic to high elevations. Reduced range and increased competition will further fragment the already isolated high elevation tree populations, which can create a genetic bottleneck (Potter et al. 2010). Many high elevation tree species are still yet to be thoroughly assessed in terms of their risk of range reduction due to climate change.

Red spruce (*Picea rubens*) is a high-elevation, late-successional, coniferous tree species that ranges from the Southern Appalachian Mountains of North Carolina to southeastern Ontario and Quebec. With a life span reaching up to 450 years, *P. rubens* serves as a foundation species in its communities, providing long-term environmental stability (Blum 1990). Red spruce is found in cool, mesic environments with acidic soils. Additionally, this species is economically valuable, serving as a source of timber and pulp, primarily used to make paper. Red spruce is also regarded as a high-quality tonewood, meaning the characteristics of its wood are excellent for use in the construction of wooden instruments (Murphy 1917). *P. rubens* provides habitat for many

species, several of which are endangered or threatened including the Virginia northern flying squirrel, the Cheat Mountain salamander, the Cow Knob salamander, and the rare lichen *Hypotrachyna virginica* (Odom et al. 2001, Dillard et al. 2008, Ford et al. 2004). Understanding the autecology of red spruce is useful for discerning the restoration potential of the species.

Red spruce has a life history that can both help and hinder its regeneration, largely depending on its life stage and surrounding environment. The seeds of red spruce trees do not persist beyond a year in the seed bank and are injured by prolonged exposure to temperatures > 33ºC in the summer months. High soil moisture levels are the primary determinant of seed germination in red spruce, with germination typically beginning in May. Seedlings grow best in dense shade which supports the cool, moist environments required for germination. However, after establishment, maximum growth rates are attained in full sun. Red spruce do not bear cones until 45 years of age and produce distinctly numerous seed crops in intervals of three to eight years. Seeds are primarily dispersed by wind up to 100 meters distance from the parent tree. Red spruce, being a shade tolerant tree, has the advantageous ability to positively respond to suppression release in advanced age and after long term suppression. This ability, coupled with its relatively long life span, allows for red spruce to become more dominant as forest succession advances (Blum 1990). However, its slow growth and time to reproductive maturity make red spruce a poor competitor in the short term. Therefore, when red spruce outcompetes faster growing hardwoods, it is due to those hardwoods being poorly adapted to the shallow and moist soils, as well as the cool temperatures of red spruce habitat, rather than any physiological advantages of red spruce (Murphy 1917). When

species, such as balsam fir (*Abies balsamea*), are well adapted to the same environments as red spruce, then red spruce can be outcompeted on a physiological basis (Dumais and Prevost 2008). The life history and physiology of red spruce are major determinants of its past range and potential future distribution

Current red spruce stands occupy only a small portion of their historical range in the Central and Southern Appalachians due to a combination of natural and anthropogenic influences. Microfossil pollen analysis suggests that the warm and dry climate of the Hypsithermal Interval between 10,000 and 5,000 B.P. is chiefly responsible for the current island-like distribution of red spruce (Bailey and Ware 1990). Post-colonization logging, human-caused forest fires, and mountain top removal mining are responsible for a further, more recent range reduction of red spruce (Pielke 1981). Fires likely lead to long-term arrested regeneration in affected populations (Blum 1990, Griscom and Griscom 2011). From the 1960's – 1980's widespread decline of red spruce was recorded throughout its range with acid rain, climate change, and winter foliar damage being proposed causes (Hamburg and Cogbill 1984, Bliss and Vogelmann 1982). Though the high elevations of the Appalachians were subjected to high levels of acid rain, investigations found that acid and heavy metal deposition levels were not high enough to cause the observed decline in red spruce (Johnson et al. 1994). Further studies suggested that the combination of acid rain and a series of severe winters resulting in extreme foliar damage were the cause of the two-decade long decline (McLaughlin et al 1987, Johnson et al 1988). While red spruce has faced declines in both the long- and short-term past, recent regeneration trends indicate a reversal in this pattern of decline (Goelz 1999, Nowacki et al. 2010).

In their current state, red spruce stands have generally stabilized from the decline of the 1960's-1980's and are mostly regenerating. Mathias and Thomas (2018) found the reversal of red spruce declines is primarily due to a decrease in acidic sulfur pollution and an increase in atmospheric CO_2. The same study found that lesser, yet significant secondary factors positively affecting red spruce regeneration are a decrease in nitrogen oxide (NO_x) pollution and an increase in spring temperatures. Likewise, Li et al. (2020) found that tree growth responded positively to temperature increases. While current warming trends have shown to be beneficial to red spruce, temperatures greater than 33ºC have proven to be injurious to red spruce seeds. Once maximum summer temperature reach or surpass this 33ºC threshold, the habitat will functionally no longer be suitable for red spruce. Seedling and sapling representation in red spruce stands indicate positive regeneration of populations in the Central and Northern Appalachians (Nowacki et al. 2010). Southern Appalachian red spruce are slightly declining in terms of growth in some areas and increasing in growth in other areas (Nowacki et al. 2010, Goelz 1999). The current regeneration trends make red spruce an ideal candidate for restoration management.

Since stabilizing from the declines of the 1960's-1980's, red spruce populations have been the subject of restoration efforts, particularly in the Central and Southern Appalachians. Growth simulations indicate that canopy thinning and small gap creation could double red spruce basal area within 50 years in West Virginia stands (Rentch et al. 2007, Rentch et al. 2010). Further, canopy thinning treatments resulting in increased understory light levels of up to 42% lead to significantly higher DBH growth and height increase in red spruce saplings and small trees when compared to controls (Rentch 2016).

Several predictive models have been used to elucidate red spruce restoration potential and to prioritize stands for management in West Virginia and the Central Appalachians (Nowacki and Wendt 2013, Beane 2010, Beane et al. 2013, Thomas-Van Gundy and Sturtevant 2014, Walter et al. 2017). HSM's implemented for West Virginia red spruce stands disagreed on the primary drivers of red spruce distribution. Nowacki and Wendt (2013) identified elevation, depth to water table, mean annual precipitation, and growing degree days as distinctly important variables, whereas Beane et al. (2013) identified maximum temperature of the warmest month and minimum temperature of the coldest month as distinctly important. Both models failed to exclude highly correlated environmental variables (e.g. temperature-related variables and elevation) which can cause multicollinearity issues in models. Multicollinearity in ENMs can influence the importance of variables (perhaps explaining discrepancies between studies) and can constrain predictions across time to correlation structures which may not remain constant over time (Guisan et al. 2017). Besides strictly mapping current distributions, ENMs have also been used to explore population specific niches and potential future distributions of red spruce.

In the Great Smoky Mountain National Park, ENMs were employed to improve the understanding of red spruce growth trends and distribution at different elevations (Koo et al. 2011). Walter et al. (2017) estimated the historical distribution of red spruce in order to create a suitability index for the central Appalachian Mountains and projected the effects of climate change on stands by the year 2100. The fundamental environmental drivers of red spruce distribution are still yet to be clearly identified. The relationship between increasing temperatures and red spruce distribution remains unclear. Modeling

the effects of climate change on red spruce distribution at more frequent time intervals may yield further insight into the relationship between temperature and red spruce distribution (Walter et al. 2017). Virginia red spruce exist in varied habitats and have an island-like distribution due to the unique physiography of the Ridge and Valley province but lack any state specific distribution or habitat suitability models.

The aim of my research is to elucidate the current restoration potential of red spruce in Virginia and investigate how climate change will affect this potential in the future. In order to address these goals, several objectives were established:

1) Model the current distribution of red spruce in Virginia using a species distribution model.

Current red spruce distribution is predicted to be primarily driven by maximum summer temperatures and average annual precipitation.

2) Model habitat suitability (the potential distribution) for Virginia red spruce and compare this data to the current distribution to determine the spatial extent to which red spruce can regenerate.

Potential red spruce suitable habitat is predicted to be greater than actual occupied habitat (i.e. the current distribution) due to recent anthropogenic disturbance.

3) Survey the red spruce populations of Virginia to elucidate the trends of red spruce regeneration (interior vs. exterior stand regeneration and elevation-related regeneration).

Red spruce is predicted to be regenerating in the majority of stands because of the reduction of air pollution stressors and warming temperatures which have not yet passed

a damaging threshold. Further, it is predicted that red spruce stands are expanding beyond current red spruce canopy cover, particularly at higher elevations.

4) Project how climate change will affect the suitable habitat available to red spruce in the future.

Climate change is expected to decrease red spruce suitable habitat by the year 2040 at the lower elevational extents of its distribution due to these lower elevations being exposed to 33ºC temperatures. By 2100, total extirpation of suitable habitat is predicted as even the highest elevations in Virginia are expected to experience dramatic warming.

METHODOLOGY

Study Area:

The Blue Ridge Mountains and Ridge and Valley province of Virginia were sampled for presence and absence points, with the state of Virginia being used as the spatial environment in which predictions were made. A presence point indicates the occurrence of red spruce at a given set of coordinates whereas an absence indicates the lack of occurrence at the location. The Blue Ridge and Ridge and Valley span the entire longitudinal extent of Virginia with presence and absence points being collected between 36° 36’ 16” N and 38° 37’ 45” N.

Habitat suitability models (HSMs) and species distribution models (SDMs) were used to address the first three aforementioned objectives. Multi-model inference (MMI), also known as ensemble modeling, was used by applying this approach both within and between algorithm types. MMI enables variance reduction in predictions by creating a

single consensus model based on the averages of constituent models. The result is a much more informed and reliable model. The R package biomod2 (v3.5.1; Thuiller et al 2009) was used to facilitate ensemble modeling predictions. The primary benefit of ensemble modeling is that it accounts for the variance present within and between algorithm types (Guisan et al. 2017).

Species Presence, True-Absence, and Pseudo-Absence Data:

Presence and absence points act as response variables in ENMs. Plots previously identified by the Virginia Department of Conservation and Recreation Division of Natural Heritage (VADCRDNH) to contain red spruce were used to locate and mark presence and absence points with a GPS device (GARMIN GPSmap 62st). Older range maps were also used as a guide to find red spruce populations (Blum, 1990). Pseudo-absence points are randomly generated absence points which serve to inform models of the full environmental gradient in the study area. Presence and true absence points were collected throughout western Virginia. A total of 338 presence points and 169 true absence points were taken. The number of presence points was greater than ten times the number of environmental variables included (n = 4) in models, but not less than 50 presence points total in order to avoid complications from sample size effects (Hernandez et al 2006, Wisz et al 2008). True absence points were purposefully collected in proximity to red spruce presence points or in areas suitable for red spruce growth to increase model discrimination. True absences were only included in the SDM to increase discrimination within models so that red spruce probability of occurrence (i.e. current distribution) would be more closely predicted rather than suitable habitat. An additional 831 pseudo-absence points (totaling to 1,000 overall absence points) were generated in

the SDM so as to not bias models by only sampling in proximity to red spruce (Wisz and Guisan 2009). For each generation of pseudo-absence points (one for the SDM and one for the HSM), three random samples were produced and used in models to reduce the influence of potentially skewed pseudo-absence sampling (Figure 1). The HSM and climate predictions lacked any true absence points and exclusively used three randomly generated iterations of 1,000 pseudo-absence points.

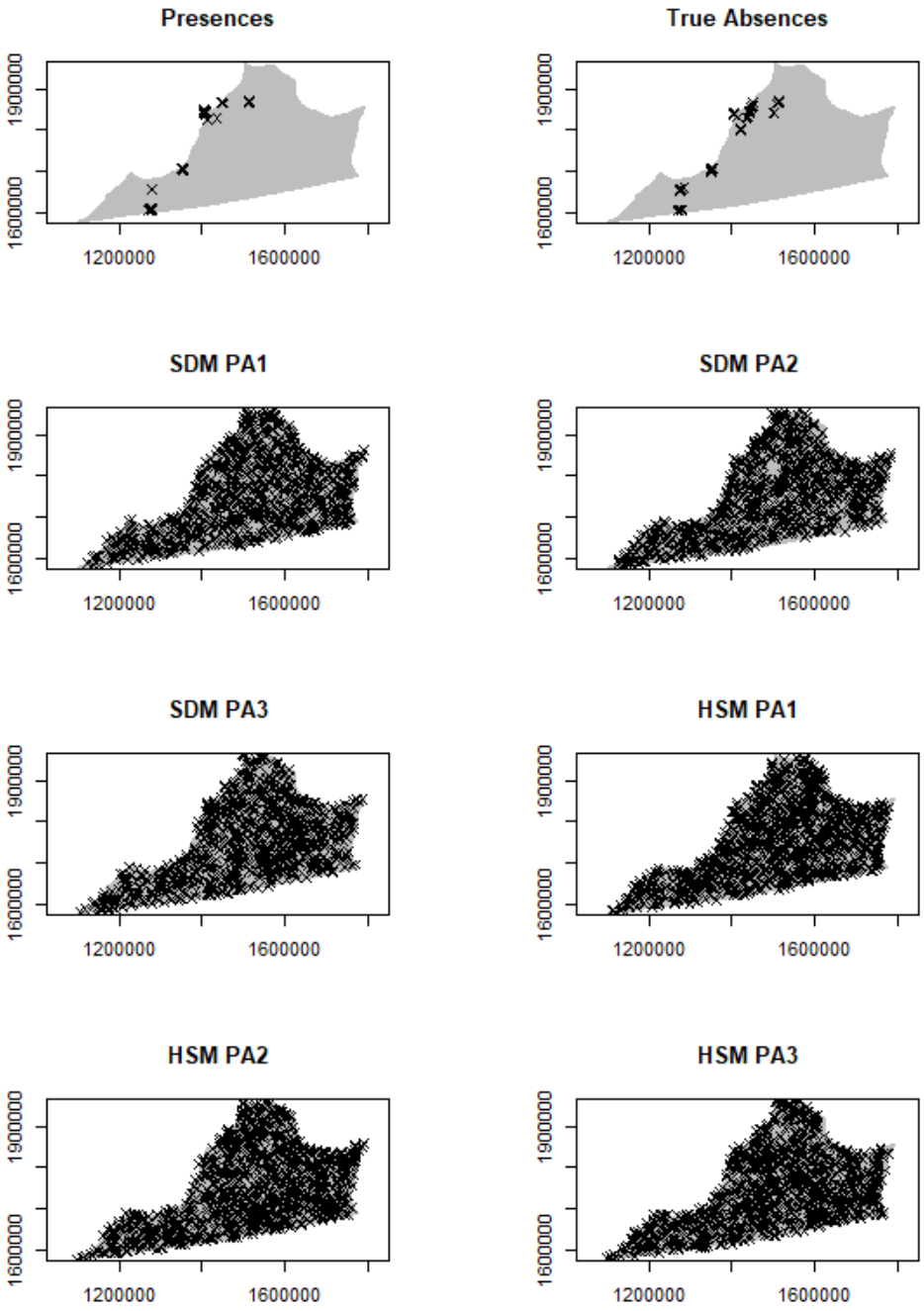

Figure 1 Presence, true-absence, and pseudo-absence (PA) samples (1 – 3) for species distribution models (SDMs) and habitat suitability models (HSMs).

Environmental Variable Selection:

A set of 93 environmental variables provided by VADCRDNH served as the predictor variables in ENMs (Table A1). These environmental variables had a 30 m x 30

m resolution and were projected in Albers Conical Equal Area in order to preserve the accuracy of area calculations. The environmental variables were assessed to eliminate redundant metrics (e.g. 1, 10, and 100 cell means of the same variable) whereby the intermediate values (i.e. 10 cell means) were kept for consideration. In order to reduce the risk of multicollinearity and identify the primary drivers of red spruce distribution, several steps were taken as a variable pre-selection process. First, environmental variables were classified as either proximal or distal. Proximal variables were those variables which more directly influence the physiology of the species (e.g. temperature), whereas distal variables had an indirect effect on red spruce physiology (e.g. elevation) (Figure 2). The most distal variables were eliminated from consideration so that the fundamental physiological drivers of red spruce distribution could be better elucidated. The remaining variables were then split into four categories: elevation derivatives, geology, precipitation, and temperature. Within each category relative importance was calculated using the importance function in biomod2. From each category only the most important variable was selected for use in models, keeping with the principle of parsimony. Finally, a variance inflation factor analysis (VIF test) was conducted on the remaining variables. A threshold of VIF score < 10 was defined, whereby any variables which exceed a score of 10 were considered too multicollinear and were therefore eliminated from consideration.

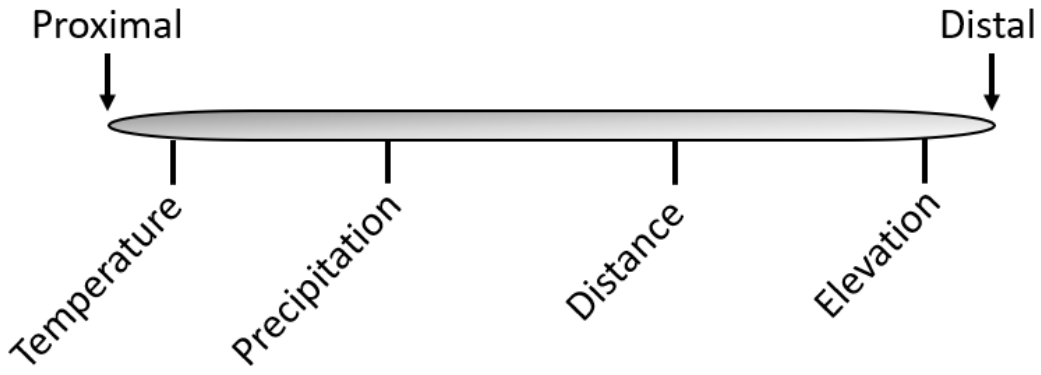

Figure 2 A spectrum describing the types of variables that may be considered proximal or distal. Temperature is proximal as it has a direct physiological effect on species, whereas elevation exclusively has indirect effects on species mediated by other, more proximal variables.

Climate Predictions:

It is common practice to project HSM's in time to investigate predicted climate change's effect on a species' suitable habitat (Thuiller 2005, Iverson et al 2008, Iverson et al 2009 Normand et al 2013, Sultana et al 2017). Projecting the effects of climate change enables land managers to make long-term plans in order to best mitigate the risk a species faces with climate change. Six ensemble models were constructed to simulate the effects of climate change on red spruce using the Canadian Earth System Model version 5 (CANESM5; Swart et al 2019). Three climate change scenarios shared socioeconomic pathway 126 (SSP126 = < 2°C warming), shared socioeconomic pathway 245 (SSP245 = < 3°C warming), and shared socioeconomic pathway 370 (SSP370 = < 4°C warming) were used to predict climate change effects on red spruce suitable habitat (http://worldclim.org). An ensemble model was generated for two of the predicted climate normal periods in the three scenarios, representing averages from 2021 – 2040 and 2081 - 2100. The HSM was used as the reference model for climate predictions with

presence and pseudo-absence points and all non-climatic variables being held constant across all climate models. Temperature and precipitation variables were altered according to the predicted climate normals for each time step. All climate prediction data was obtained from worlclim.org. Climate prediction rasters were imported into ArcGIS Pro v – (ESRI, Redlands, CA), where they were cropped to the extent of Virginia, resampled to a 30 m x 30 m resolution using bilinear sampling, and projected to Albers Conical Equal Area in order to match the raster data obtained from VADCRDNH. Species range change (SRC) is a function of the biomod2 package that allows for a calculation to be made of the percent area increase or decrease of habitat suitability given a climate change scenario. This is done by first converting the current HSM, as well as the climate prediction HSMs into a binary format where zero equals unsuitable habitat and one equals suitable habitat. The binary climate models are then individually overlayed on the current HSM binary model after which each cell in the respective model's raster environment is classified as stable suitable (1 to 1), stable unsuitable (0 to 0), suitable to unsuitable (1 to 0), or unsuitable to suitable (0 to 1) which yields a percent change for each classification. SRC was used to track trends exhibited by red spruce habitat suitability in response to climate change scenarios.

Algorithm Parameterization:

Four modeling algorithms were used in each modeling objective in this study: generalized linear models (GLMs), generalized additive models (GAMs), randomforests (RFs), and boosted regression trees, referred to as generalized boosted models (GBMs) in biomod2. GLMs are parametric logistic regression algorithms in which assumptions must be made about the shape of response curves prior to running models (Guisan et al.

2017). The GLMs used in this study were parameterized to have polynomial terms and an interaction level of one in order to account for first and second order effects, as well as potential interaction unaccounted for in the VIF test. GLM equations were automatically generated using a stepwise procedure that evaluates and compares the Akaike information criterion score (AIC) of each equation to generate most parsimonious algorithm. GAMs primarily differ from GLMs in that they are semi-parametric, meaning they do not require any assumptions about the shape of response curves prior to running models. Using the mgcv package (v1.8-33), GAMs made use of smoothing splines which fit response curves to data without a priori postulation of the shape of the response curve being necessary (Wood 2006). Equations for GAMs were generated automatically using a similar stepwise procedure as the GLMs where AIC scores were used to identify the most parsimonious equations. RFs are algorithms that use recursive partitioning (i.e. decision trees) in order to relate presence and absence data to environmental variables. Rather than generating one single tree, which is a high variance process, RFs generate multiple trees by randomly resampling a portion of the original dataset and then averaging the resulting trees, a statistical method known as bootstrapping (Breiman 2001). For each individual RF algorithm 500 trees were generated via bootstrapping. GBMs likewise take a recursive partitioning approach, however, GBMs use an iterative process where new trees are generated and fitted to the residuals of the previously generated trees, a statistical method known as boosting (Ridgeway, 1999). To determine the ideal number of trees to use for GBMs a “pruning” method was used. This method generates an enormous number of trees (e.g. 10,000 in this case), then measures at what number of trees model performance no longer improves. GBMs achieved maximum performance around 6,000

trees. All other aspects of individual algorithm parameterization were left to the default settings in biomod2 (v3.5.1).

Ensemble Model Parameterization:

Eight total ensemble models were generated in this study accounting for the SDM, HSM, and six climate models. Ensembles used a cross-validation procedure where three evaluation runs of the models were conducted, with each model run being calibrated using a randomly selected subset of 80% of data which was then evaluated on the remaining 20% of data. Each ensemble also ran three additional times for each of the three pseudo-absence selections. Therefore, each individual ensemble model contained 36 different individual models (4 algorithms x 3 evaluation runs x 3 pseudo-absence selections). Within each ensemble model three types of averages were calculated. The first type of average was a simple mean of predictions across the 36 individual models. The second type of average was weighted based on model evaluation scores, whereby a higher evaluation score led to a corresponding high weight when calculating averages. The final average was a committee average, which uses binary prediction maps from each of the 36 individual models generated by assessing the highest quality predictions as the basis for calculating averages. The mapped prediction values from the representative HSM ensemble models were binned using the following habitat classification scale in order to better visualize map projections: unsuitable 0.00 – 0.20; poor 0.21 – 0.40; fair 0.41 – 0.60; good 0.61 – 0.80; excellent 0.81 – 1.00. The SDM ensemble map predictions were binned using the same intervals, however, values represent a probability of occurrence as opposed to habitat quality: not present 0.00 – 0.20; low occurrence

probability 0.21 – 0.40; intermediate occurrence probability 0.41 – 0.60; good occurrence probability 0.61 – 0.80; high occurrence probability 0.81 – 1.00.

Model Evaluations:

Models were evaluated based on the true skill statistic (TSS) and area under the receiver operating characteristic curve (AUC of the ROC or simply ROC). The TSS is a model evaluation based on Cohen's kappa, however, the TSS is adjusted so that prevalence of the species no longer affects evaluation scores as is the case with kappa. TSS and kappa both fall into the calibration category of evaluation metrics, meaning they measure a model's ability to correctly predict the conditional probability of presence, given the condition of the environmental variables. The ROC, on the other hand, is a discrimination metric, meaning it measures the ability of a model to distinguish between occupied and unoccupied sites (Phillips and Elith 2010). Because TSS and ROC are measuring different aspects of model performance, it is useful to consider both when deciding which individual models should be included in an ensemble. TSS scores range from zero to one, with the following scale used to assess model performance: poor 0.00 – 0.20; fair 0.21 – 0.40; moderate 0.41 – 0.60; substantial 0.61 – 0.80; excellent 0.81 – 1.00 (Landis and Koch 1977). ROC scores likewise range from zero to one with a slightly different evaluation scale: counter-predictions ROC < 0.50; fail 0.51 – 0.60; poor 0.61 – 0.70; fair 0.71 – 0.80; good 0.81 - 0.90; excellent 0.91 – 1.00 (Guisan et al. 2017). A threshold of TSS > 0.80 and ROC > 0.90 was defined whereby all individual models which fell under these limits were eliminated from ensemble predictions. Ensemble models were evaluated based on the TSS as well as the sensitivity (rate of correctly identifying presence/suitable habitat) and specificity (rate of correctly identifying

absence/unsuitable habitat) of models. Of the three ensemble averages calculated, the type with the highest sensitivity and specificity scores were selected as representatives. Response curves were generated for each of the environmental variables in the SDM and HSM using the evaluation strip method in biomod2. The evaluation strip method produces response curves by generating a set of predictions by a model where only one environmental variable is allowed to vary, and the remaining environmental variables are held constant (Elith et al 2005).

Regeneration Surveys:

While SDMs and HSMs provide practically useful spatial predictions, they do not include data on the regeneration trends of the modeled species. The regeneration trends of a species were used in concert with suitability and distribution models to determine the restoration potential of the species. Therefore, this study aims to complement the ENMs with data on the regeneration trends that are present in red spruce populations.

The relationship between elevation and regeneration as well as comparisons of regeneration in the interior versus exterior portions of red spruce stands were measured by a series of plots. In order to be considered for the regeneration survey, a red spruce stand must have had 10 reproductive adults (as determined by cone presence on trees or a DBH > 30 cm) present within a 30 m radius. Stands which had less than 10 reproductive adults within a 30 m radius often were too small or mixed to be sampled. Candidate sites were visited in most regions where red spruce in known to occur in Virginia, including Shenandoah National Park, the Shenandoah Mountains, Highland County, Beartown Wilderness Area, Mountain Lake Wilderness Area, Grayson Highlands State Park, Mount Rogers, and Whitetop Mountain. Four sites across Virginia were selected to be

surveyed at Highland County (n = 2), Mount Rogers (n = 1), and Whitetop Mountain (n = 1) (Figure 3). At each site an initial 40m long transect was randomly placed perpendicular to the edge of a red spruce stand so half of the transect's length was in the interior of the forest and the other half was in the exterior of forest (Figure 4). From this initial transect a nested plot design was made. Within 1 meter of the transect line, all red spruce seedlings (DBH < 1 cm) were counted. Within 3 meters of the transect line, all red spruce saplings (DBH < 15 cm) were counted. Within 10 meters of the transect line all adult trees (DBH > 15 cm) were counted (Figure 4). From the initial nested plot, the edge of the forest was followed whereby an additional 11 plots were placed at least 70 meters apart from each other. The elevation was recorded at the center of each plot. In RStudio (v1.3.1093) Kruskal-Wallis and Mood's Median tests were conducted to compare (1) exterior vs. interior counts within life-stage cohorts, (2) seedling exterior vs. interior counts by site, and (3) seedling to sapling count ratios by site and position. A linear regression analysis was also conducted to determine the relationship between regeneration at each life-stage and elevation.

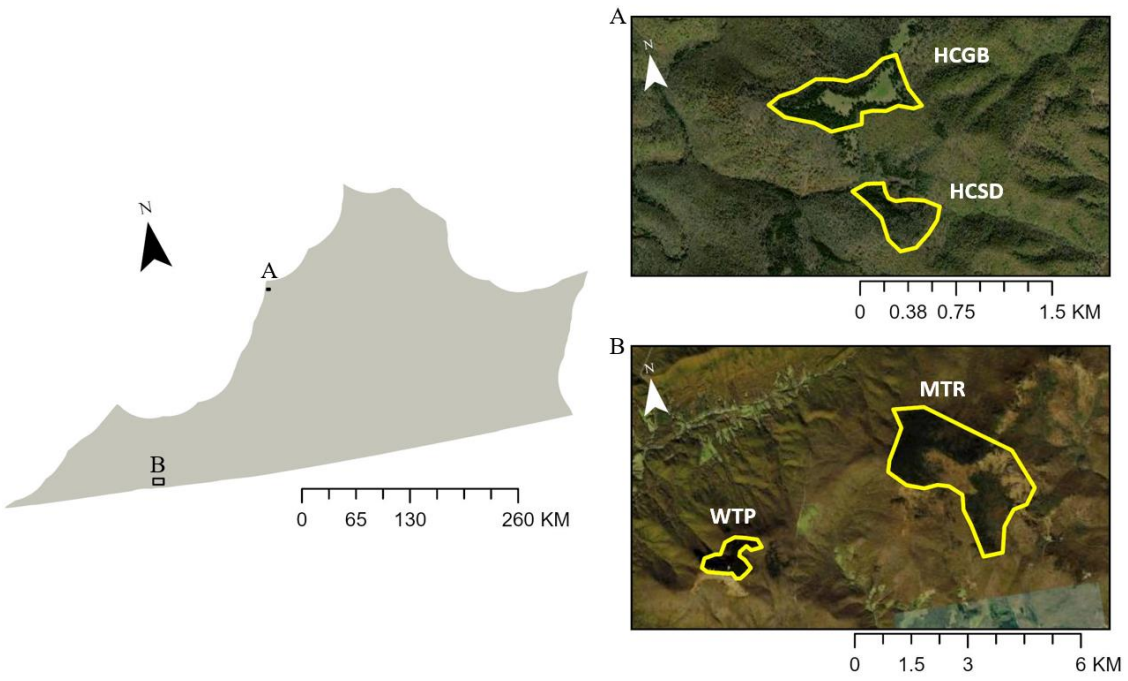

Figure 3 Satellite images of A) Central Appalachian regeneration survey sites at Highland County grassy bald (HCGB) and Highland County stand (HCSD) and B) Southern Appalachian survey sites at Whitetop Mountain (WTP) and Mount Rogers (MTR).

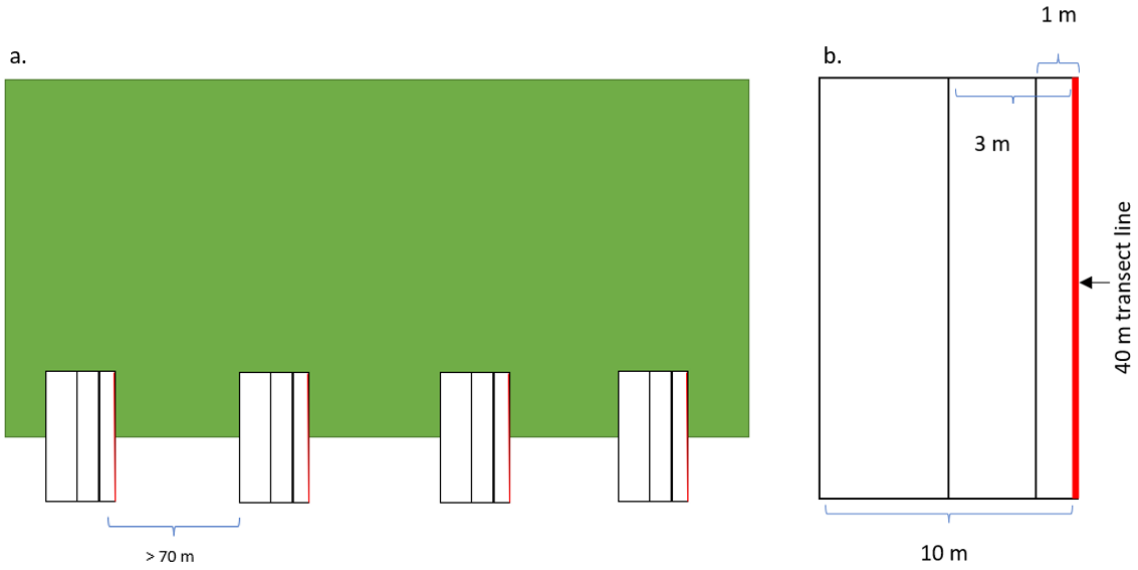

Figure 4 Regeneration survey design; a) regeneration survey plots along the edge of a red spruce stand (in green) and b) nested plot design for sampling different stage-cohorts.

RESULTS

Environmental Variable Selection:

The most important environmental variables from the elevation derivatives, geology, precipitation, and temperature categories were maximum temperature of the warmest month (MxTpWrmMth), May precipitation (MayPrecip), total insolation derived from direct and diffuse, but not reflected, radiation for the summer solstice (radsumsol), and distance to acidic shale bedrock (geo200). The generalized linear model (GLM) importance values were ignored for average calculations in the temperature and geology categories due to some variables being excluded from equations resulting in values of zero. Other algorithms featured zero values for variable importance, however these zero values resulted from rounding rather than exclusion from equations and were therefore considered when calculating averages across algorithms. Both MxTpWrmMth and minimum diurnal range (MnDiurnRng) had an average importance of 0.30, however, MxTpWrmMth was selected as it is the more proximal variable of the two (Table A2). A variance inflation factor analysis (VIF) test indicated that there were no multicollinearity issues between any of the four variables (Table 1). Across the species distribution models (SDMs) and habitat suitability models (HSMs) MxTpWrmMth was the most important variable followed by either MayPrecip or geo200 depending on the model, and lastly radsumsol (Table 2).

Table 1 Variance inflation factor analysis (VIF) scores of the four environmental variables included in models: average May precipitation (MayPrecip), maximum temperature of the warmest month, insolation during the summer solstice (radsumsol), and distance from acidic shale bedrock (geo200).

Variable	VIF score
MayPrecip	2.619012
MxTpWrmMth	1.631448
radsumsol	1.682212
geo200	1.936584

Table 2 Raw mean importance in species distribution models (SDMs) and habitat suitability models (HSMs) of utilized environmental variables: average May precipitation (MayPrecip), maximum temperature of the warmest month, insolation during the summer solstice (radsumsol), and distance from acidic shale bedrock (geo200).

Variable	Model Type	GLM	GAM	RF	GBM	Mean
MxTpWrmMth	SDM	0.91	0.57	0.77	0.95	0.80
MayPrecip	SDM	0.06	0.47	0.10	0.05	0.17
geo200	SDM	0.22	0.22	0.08	0.02	0.14
radsumsol	SDM	0.08	0.03	0.06	0.03	0.05
MxTpWrmMth	HSM	0.86	0.81	0.76	0.96	0.85
MayPrecip	HSM	0.07	0.30	0.08	0.01	0.11
geo200	HSM	0.29	0.20	0.06	0.00	0.14
radsumsol	HSM	0.01	0.02	0.00	0.00	0.01

Species Distribution Models:

With the exception of two generalized linear models (GLMs), all individual models in the SDM ensemble had a true skill statistic score (TSS) > 0.80 and an area under the receiver operating characteristic curve score (ROC) > 0.90, indicating excellent predictions. Two GLMs had a 0.80 > TSS > 0.60 and a 0.90 > ROC > 0.80 and were therefore excluded from ensemble predictions (Table A3). Randomforests (RFs) had the highest overall TSS and ROC scores, followed by generalized boosted models (GBMs), generalized additive models (GAMs), and GLMs (Figure 5). Response curves showed strong agreement both within and across algorithm type (Figure 6). For MxTpWrmMth, probability of occurrence was highest at approximately 24°C and decreased with increased temperature with a severe decline to a probability of zero occurring around 26°C across all models. At temperatures below 22°C, probability of occurrence dropped precipitously. Response to MayPrecip was positive as precipitation increased. A noticeable increase in probability of occurrence occurred around 110 mm and typically peaked with the highest precipitation amounts of about 200 mm. geo200 typically only featured perturbations in response at distances between zero and 5,000 meters, although the extent and location of perturbation varied greatly between algorithms. Generally, probability of occurrence decreased as distance increased, but quickly rebounded at approximately 2,500 meters. Radsumsol response plots showed a negative relationship between occurrence probability and insolation. Probability of occurrence typically decreased between 30 and 35 kilowatt hours per square meter (kWh/ m^2) (Figure 6). SDM ensemble predictions were excellent with TSS and ROC scores > 0.90. The

committee average was selected to be the representative model, as it had the highest sensitivity and specificity amongst the ensemble predictions (Figure 7, Table 3).

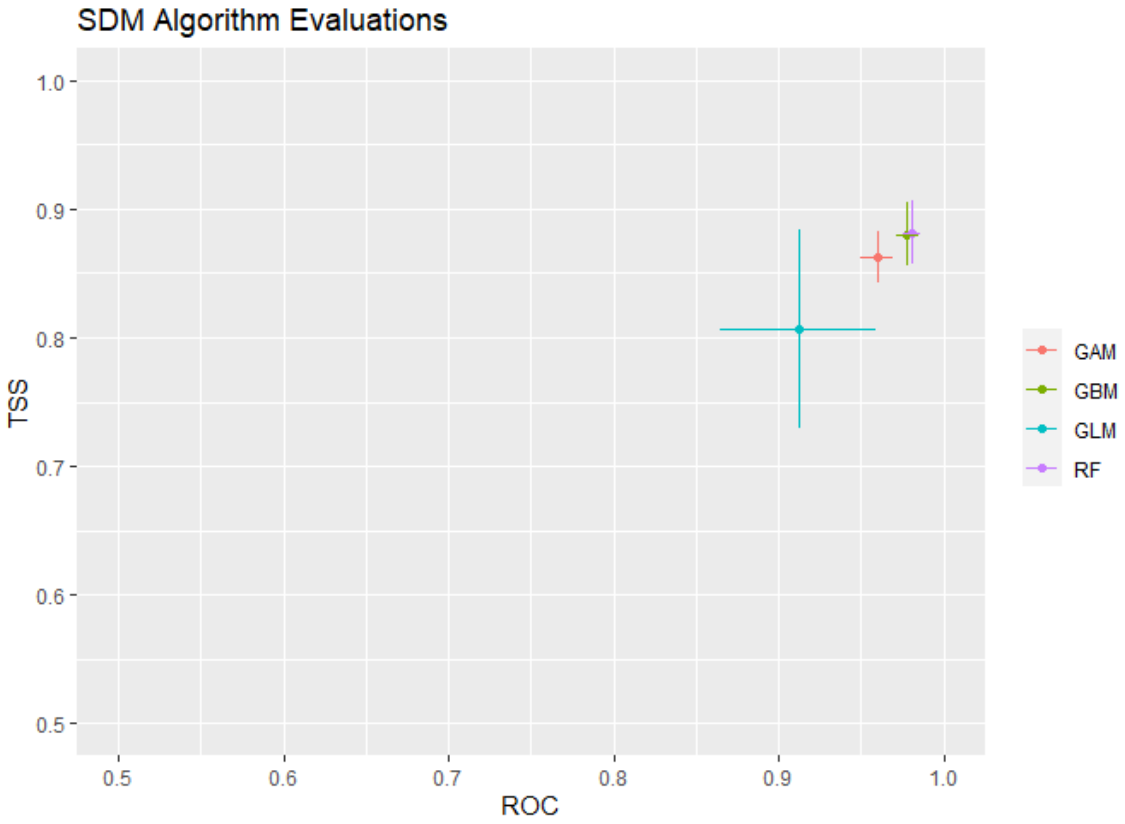

Figure 5 Species distribution model (SDM) true skill statistic (TSS) and area under the receiver operating characteristic curve (ROC) scores by algorithm type; generalized additive model (GAM), generalized boosted model (GBM), generalized linear model (GLM), and Randomforest (RF).

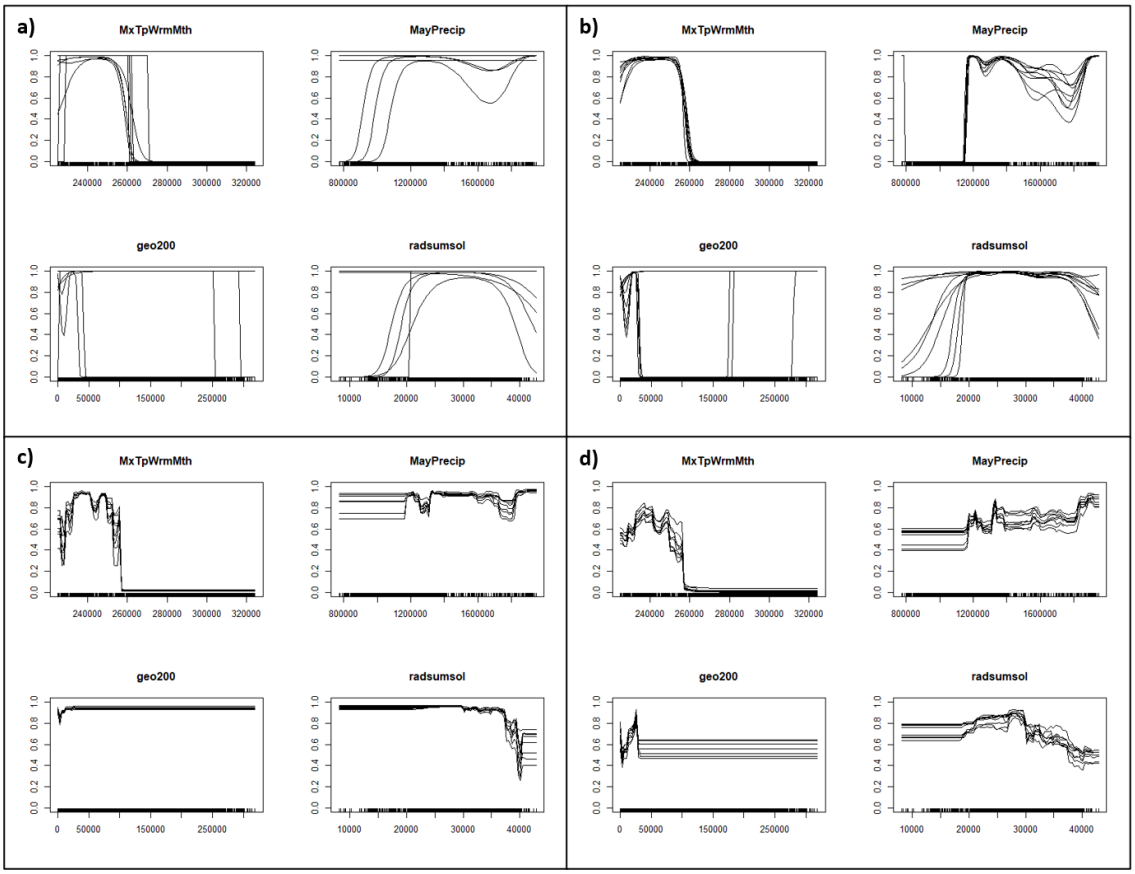

Figure 6 Species distribution model response in terms of probability of red spruce occurrence (y-axes) for each environmental variable gradient (x-axes) in a) generalized linear models, b) generalized additive models, c) generalized boosted models, and d) Randomforest models.

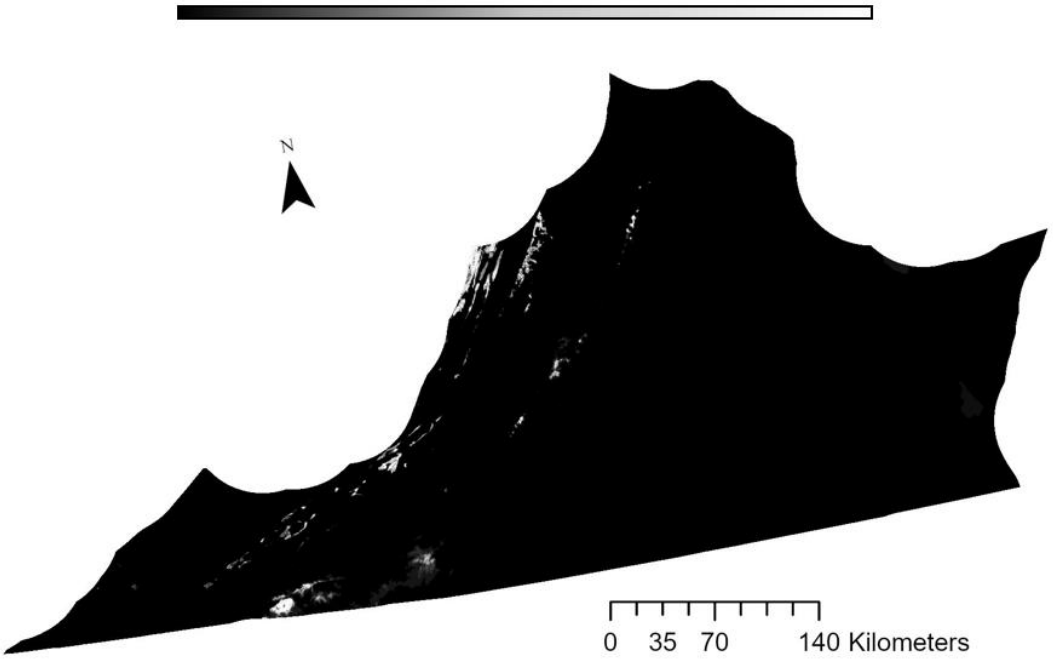

Figure 7 Committee average ensemble species distribution model map projection; probability of occurrence is displayed from 0 (black) – 1 (white) with gray indicating intermediate values.

Table 3 Species distribution ensemble models evaluations including overall model evaluations (testing data), integerized prediction probability cutoff values for constructing binary maps (cutoff), rate of correctly identifying presence (sensitivity), and rate of correctly identifying absence (specificity). Scores arranged by kappa, true skill statistic (TSS), and area under the receiver operating characteristic curve (ROC).

Ensemble Model	Evaluation Metric	Testing data	Cutoff	Sensitivity	Specificity
Raw Average	KAPPA	0.938	779.0	93.195	99.437
	TSS	0.957	679.0	97.041	98.685
	ROC	0.988	626.5	97.633	98.159
Weighted Average	KAPPA	0.938	711.0	96.154	99.023
	TSS	0.958	681.0	97.041	98.723
	ROC	0.988	624.5	97.633	98.159
Committee Average	KAPPA	0.957	929.0	95.858	99.549
	TSS	0.963	869.0	97.041	99.286
	ROC	0.999	867.5	99.041	99.286

Habitat Suitability Models:

All individual models in the HSM ensemble had a TSS > 0.80 and ROC > 0.90, indicating excellent predictions. Two individual GAMs, GAMRun1PA2 and GAMRun3PA3, exhibited clear overfitting which occurs when a model fits exactly to the training data (Tables A4). The result of overfitting is a model which cannot make predictions beyond the scope of the training data and can cause map projections to be overly restrictive and nearly binary (Figure 8). TSS and ROC scores exhibited minimal variation between algorithms, with RFs having the highest overall scores (Figure 9) . Response curves show fairly strong agreement across algorithms, although some individual models within the GLM and GAM algorithms disagreed. In some of the GLM and GAM equations, certain environmental variables were deemed too unimportant to include, which results in a flat horizontal line across the entire extent of the environmental spectrum in response plots at a response value of 1.0. The RF response curves of the HSM are fairly similar to those seen in the SDM. The HSM GBM response curves for MxTpWrmMth are nearly identical to that of the SDM, however the response curves of the remaining three variables are notably muted in terms of perturbation compared to the SDM curves. Across all algorithms in the HSM, radsumsol generally lacks a decline in probability of occurrence at the upper extreme values as was observed with the SDM (Figure 10). HSM ensemble predictions were excellent with TSS > 0.90. The committee average was selected to be the representative model, as it had the highest sensitivity and specificity (Figure 11, Table 4). A binary HSM map projection was generated from the non-binary committee average map projection using TSS scores whereby all cells with a TSS value greater than or equal to 960 were identified as suitable

habitat (1) and all values less than 960 were identified as unsuitable habitat (0) (Figure 12, Table 4).

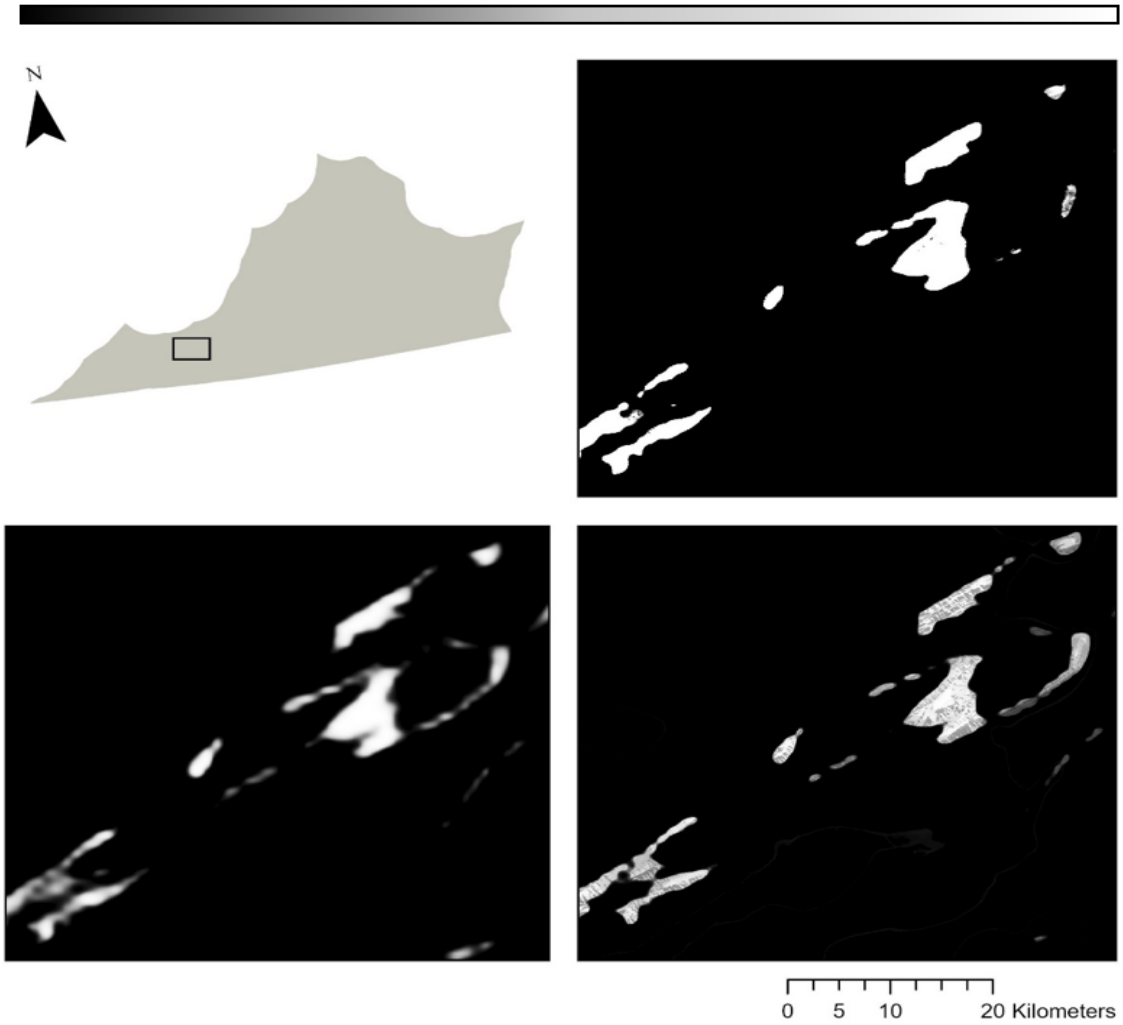

Figure 8 Visual comparison of a nearly binary overfitted generalized additive model (top right) with a normally fit generalized linear model (bottom left) and randomforest model (bottom right) in southwestern Virgnia (top left); probability of suitable habitat is displayed from 0 (black) – 1 (white) with gray indicating intermediate values.

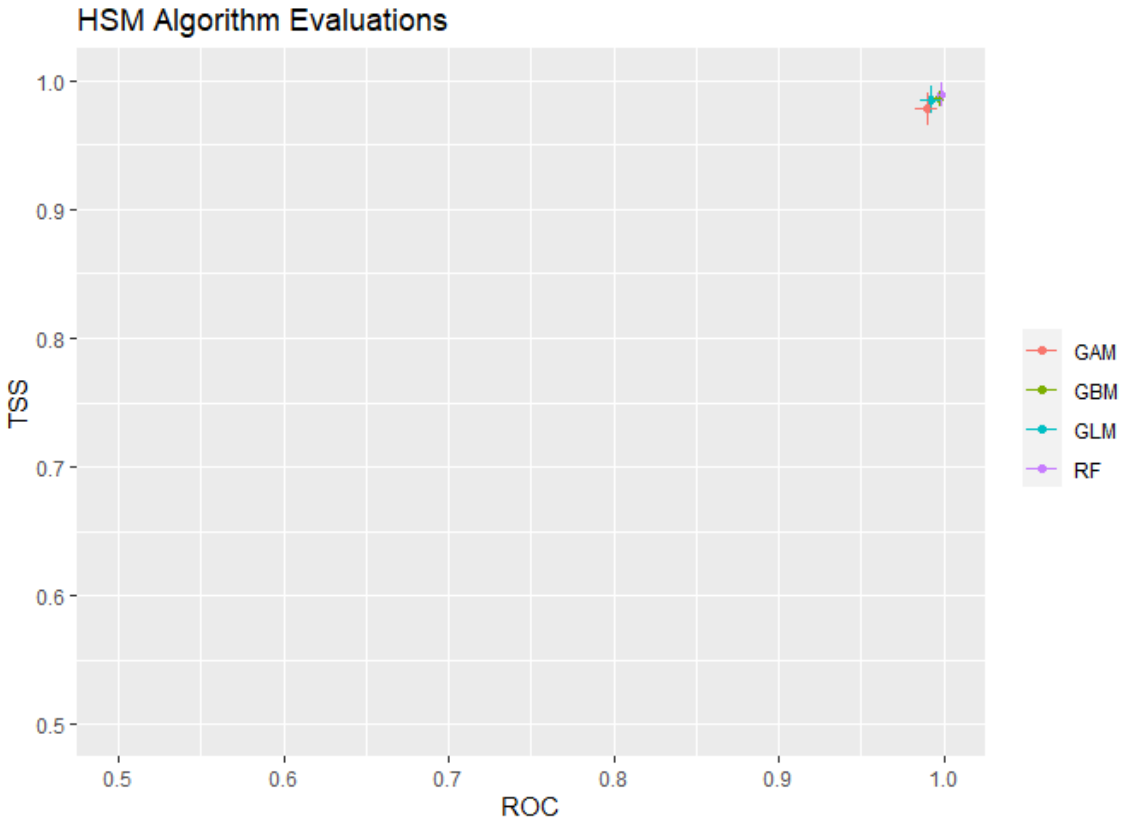

Figure 9 Habitat suitability model (HSM) true skill statistic (TSS) and area under the receiver operating characteristic curve (ROC) scores by algorithm type; generalized additive model (GAM), generalized boosted model (GBM), generalized linear model (GLM), and Randomforest (RF).

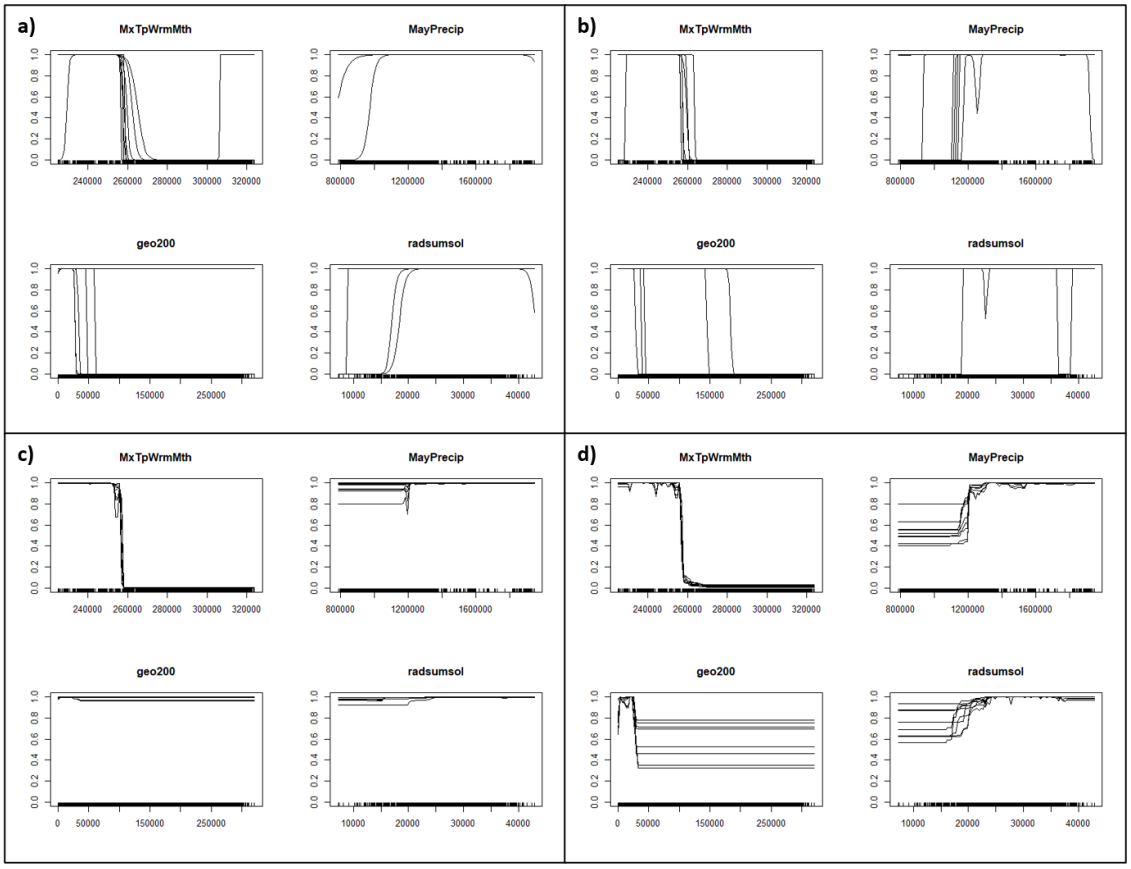

Figure 10 Habitat suitability model (HSM) response in terms of probability of suitable habitat (y-axes) for each environmental variable gradient (x-axes) in a) generalized linear models, b) generalized additive models, c) generalized boosted models, and d) Randomforest models.

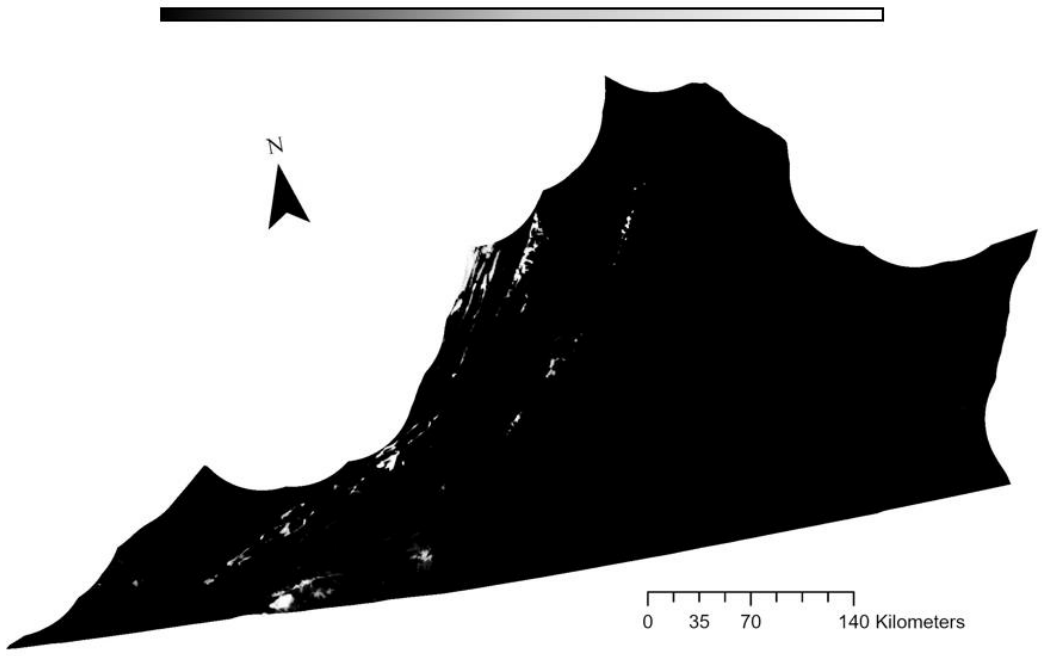

Figure 11 Committee average ensemble habitat suitability model map projection; probability of suitable habitat is displayed from 0 (black) – 1 (white) with gray indicating intermediate values.

Table 4 Habitat suitability ensemble models evaluations including overall model evaluations (testing data), integerized prediction probability cutoff values for constructing binary maps (cutoff), rate of correctly identifying suitable habitat (sensitivity), and rate of correctly identifying unsuitable habitat (specificity). Scores arranged by kappa, true skill statistic (TSS), and area under the receiver operating characteristic curve (ROC).

Ensemble Model	Evaluation Metric	Testing data	Cutoff	Sensitivity	Specificity
Raw Average	KAPPA	0.990	893.0	99.408	99.867
	TSS	0.996	797.0	100.000	98.567
	ROC	1.000	797.0	100.000	98.567
Weighted Average	KAPPA	0.990	894.0	99.867	99.867
	TSS	0.995	798.0	100.000	98.533
	ROC	1.000	802	100.000	99.567
Committee Average	KAPPA	0.993	960.0	99.704	99.9
	TSS	0.996	960.0	99.704	99.9
	ROC	1.00	958.0	99.704	99.9

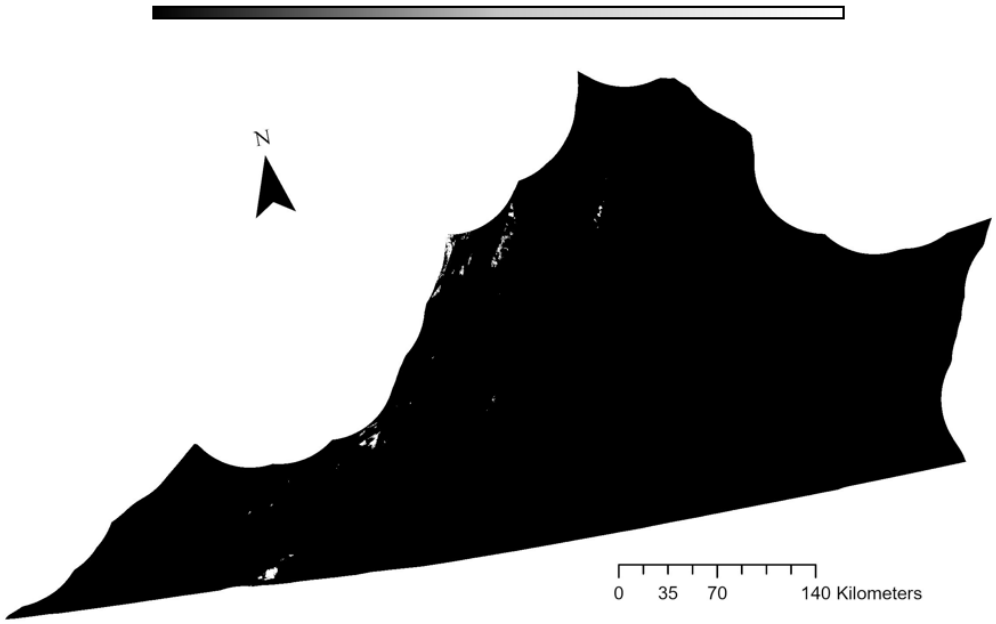

Figure 12 Committee average ensemble habitat suitability model map projection transformed to a binary format where black (0) is unsuitable habitat and white (1) is suitable habitat.

Species Distribution Models versus Habitat Suitability Models:

For both the SDM and HSM the 0.0 – 0.2 bins accounted for the most area when compared to the other bins (Table 5). This represents the fact that the vast majority of area in Virginia is not occupied by and is unsuitable for red spruce. The SDM accounts for a much greater area in the 0.2 – 0.4 bin compared to the HSM area. In the 0.4 – 0.6 and 0.6 – 0.8 bins, areas are relatively even with the SDM having a slightly greater number of hectares in both instances. In the 0.8 – 1.0 bin the HSM has a much greater area when compared to the SDM (Figure 13). A visual comparison of the SDM and HSM in southwestern Virginia shows the increased discriminatory ability of the SDM, while both models are able to identify and agree on broadly unoccupied/unsuitable habitat (Figure 14).

Table 5 Area (in hectares) occupied by each probability bin between the species distribution model (SDM) and habitat suitability model (HSM).

Bin	SDM Area (ha)	HSM Area (ha)
0.0 – 0.2	11271100.32	11269827.45
0.2 – 0.4	42422.49	29505.96
0.4 – 0.6	30964.50	24998.04
0.6 – 0.8	28529.19	29073.60
0.8 – 1.0	44040.51	63651.96

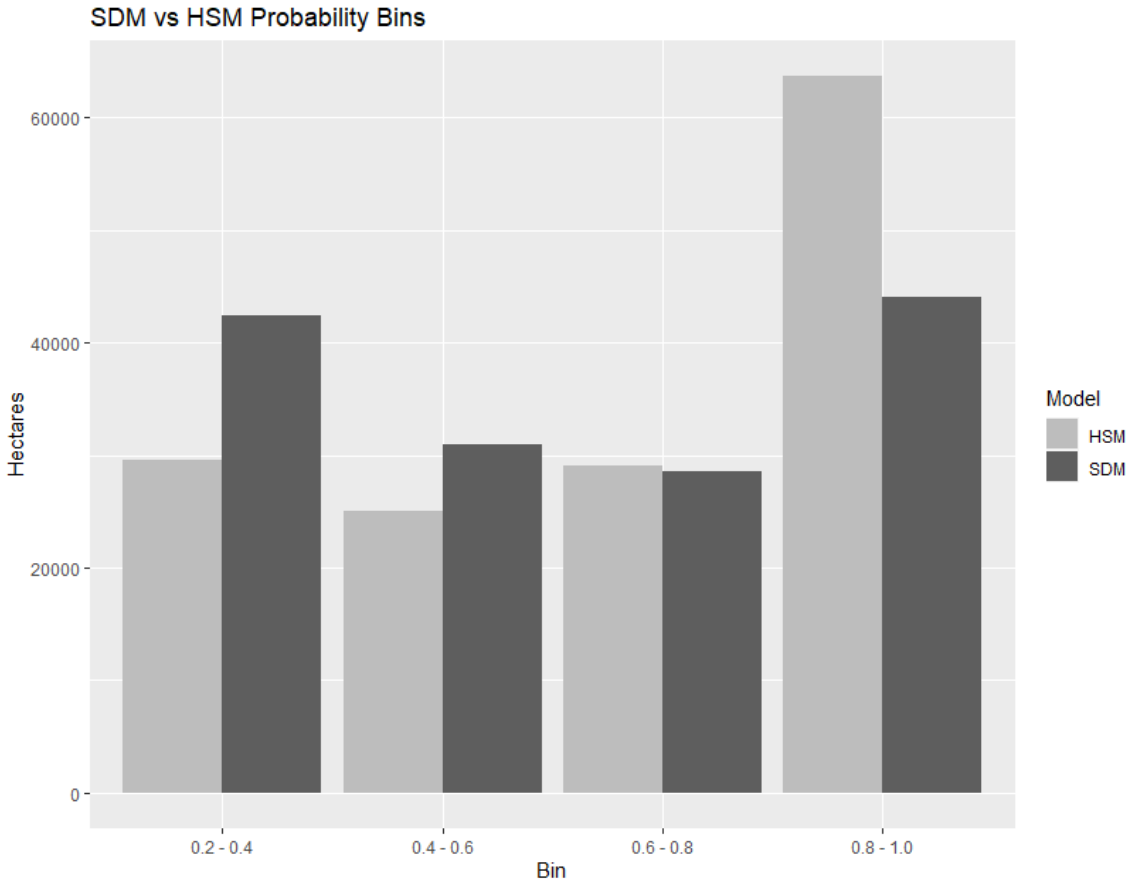

Figure 13 Comparison of areas occupied by each probability bin in the ensemble species distribution model (SDM; dark gray) and ensemble habitat suitability model (HSM; light gray).

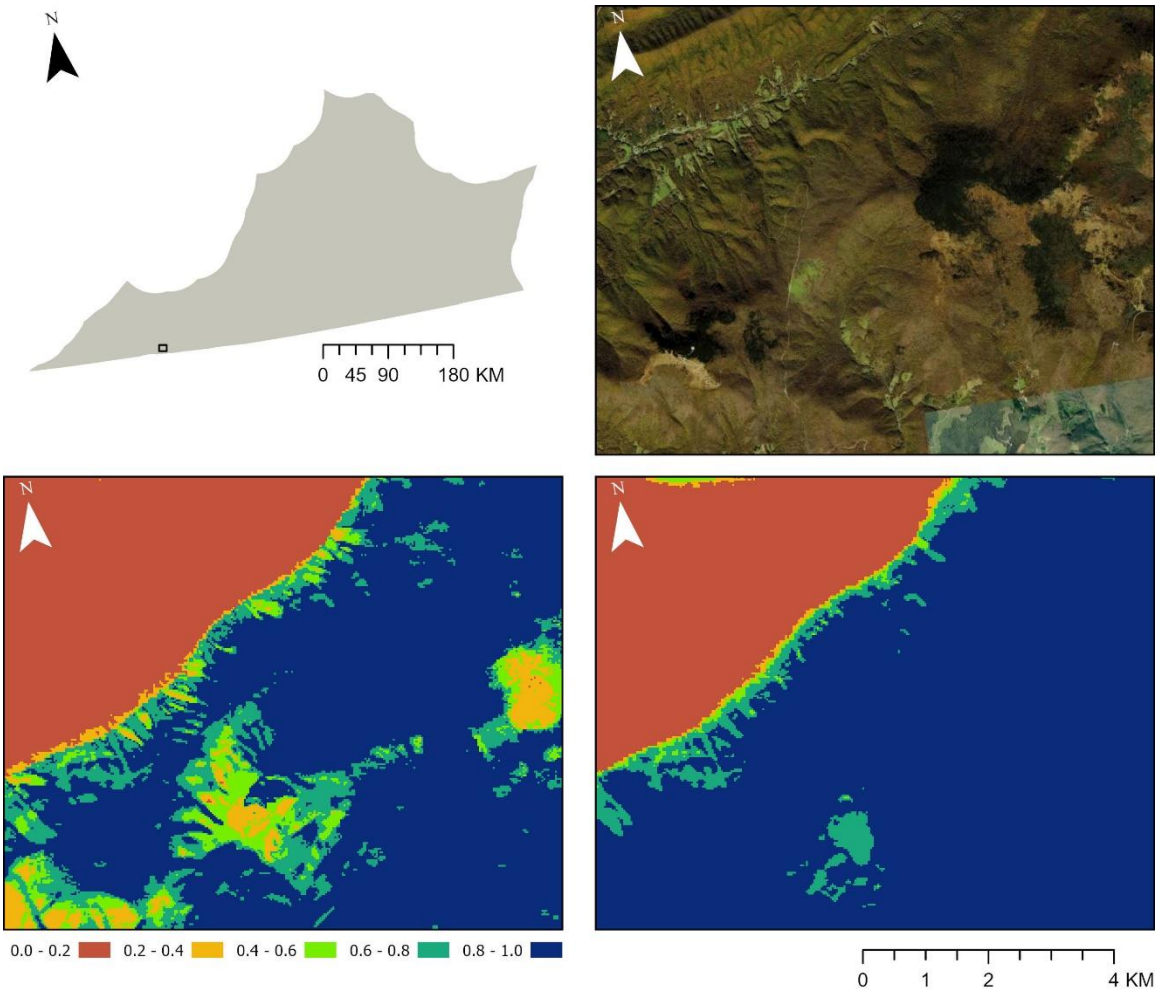

Figure 14 Visual comparison of satellite imagery (top right), the ensemble species distribution model (SDM; bottom left), and ensemble habitat suitability model (HSM; bottom right).

Regeneration Surveys:

Across site, significant differences were only seen between seedling counts ($p = 0.04908$) (Figure 15). However, a pairwise analysis within seedling counts across sites revealed no significant differences between the Highland County grassy bald site (HCGB) and the Whitetop Mountain site (WTP) ($p = 0.08$). The sapling ($p = 0.3269$) and adult ($p = 0.3109$) cohorts showed no significant differences across sites. Summed counts across all cohorts showed no significant differences ($p = 0.06404$) (Figure 15).

Figure 15 Counts across sites in seedlings (Kruskal-Wallis, p = 0.04908; top left), saplings (Mood's Median Test, p = 0.3269; top right), adults (Kruskal-Wallis, p = 0.3109; bottom left), and sum totals across cohorts (Mood's Median Test, p = 0.06404; bottom right). Site names from left to right in each graph; Highland County Grassy Bald (HCGB), Highland County Stand (HCSD), Mount Rogers (MTR), Whitetop Mountain (WTP).

Interior red spruce counts were significantly higher in the adult ($p < 0.0001$) and sapling ($p = 0.03$) cohorts when compared to their respective exterior cohort counts, but there was no significant difference in the seedling cohort ($p > 0.1$; Figure 16). Seedling counts were analyzed by site and stand position (interior vs. exterior) to further investigate the lack of difference in the seedling cohort. Comparison between seedling counts and overall site and position indicate significant differences ($p = 0.01794$). However, pairwise comparisons of seedling counts by site and position revealed no

significant differences within or between sites (p > 0.05) (Figure 17). While no significant differences were present in seedlings by site and position, WTP interior has a considerably greater median than all other sites and positions and HCGB exterior has a slightly greater median (median = 500) than HCGB interior (median = 0) (Figure 17).

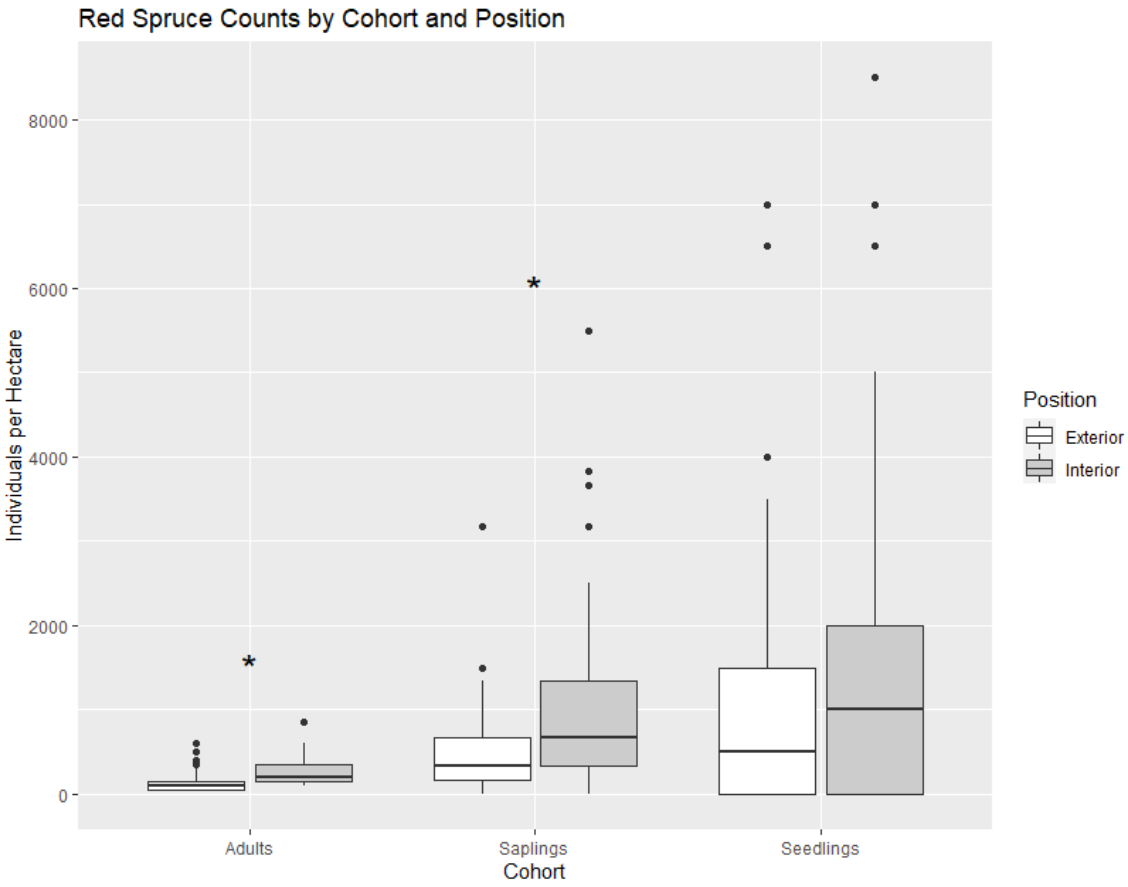

Figure 16 Counts by cohorts and position. Significant differences within cohort are denoted by * in adults (p < 0.0001) and saplings (p = 0.03).

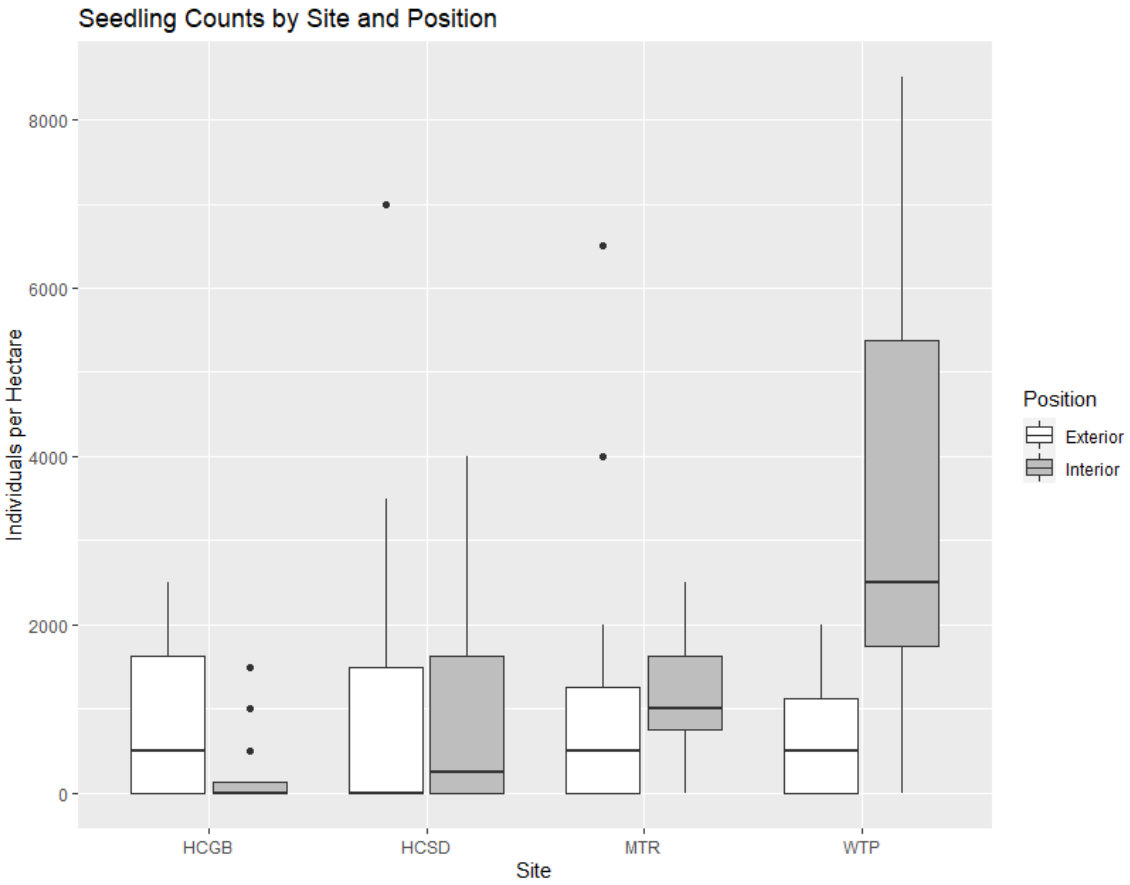

Figure 17 Seedling counts by site and position with significant differences; Significant differences exist when comparisons are made with the overall dataset (p = 0.01794), however no pairwise significant differences exist (p> 0.05). Site names from left to right in each graph; Highland County Grassy Bald (HCGB), Highland County Stand (HCSD), Mount Rogers (MTR), Whitetop Mountain (WTP).

There were no significant differences in the seedling to sapling ratios across sites and position ($p > 0.1$). All median ratio values were < 3 (Figure 18). Seedling and sapling counts were similar to that of Nowacki et al (2010) conducted in the Central and Southern Appalachian Mountains (Table 6). No strong relationships were found between seedlings and elevation ($p = 0.0361$, $R^2 = 0.03576$), saplings and elevation ($p = 0.0325$, $R^2 = 0.03758$), adults and elevation ($p = 0.7903$, $R^2 = -0.0089874$), or total red spruce counts and elevation ($p = 0.0158$, $R^2 = 0.05045$) (Figure 19).

Figure 18 Seedling to sapling ratios by site and position. Site names from left to right in each graph; Highland County Grassy Bald (HCGB), Highland County Stand (HCSD), Mount Rogers (MTR), Whitetop Mountain (WTP).

Table 6 Comparisons of average seedling and sapling counts from this study's sites (HCGB = Highland Count grassy bald, HCSD = Highland County stand in this study, MTR = Mount Rogers, WTP = Whitetop Mountain) and values from Nowacki et al (2010) arranged by Appalachian region.

Region	Site and Cohort	Study Individuals per hectare	Literature Individuals per hectare
Central Appalachians	HCGB Seedlings	583	8713
	HCGB Saplings	563	563
	HCSD Seedlings	1208	8713
	HCSD Saplings	632	563
Southern Appalachians	MTR Seedlings	1208	1599
	MTR Saplings	542	376
	WTP Seedlings	2063	1599
	WTP Saplings	1347	376

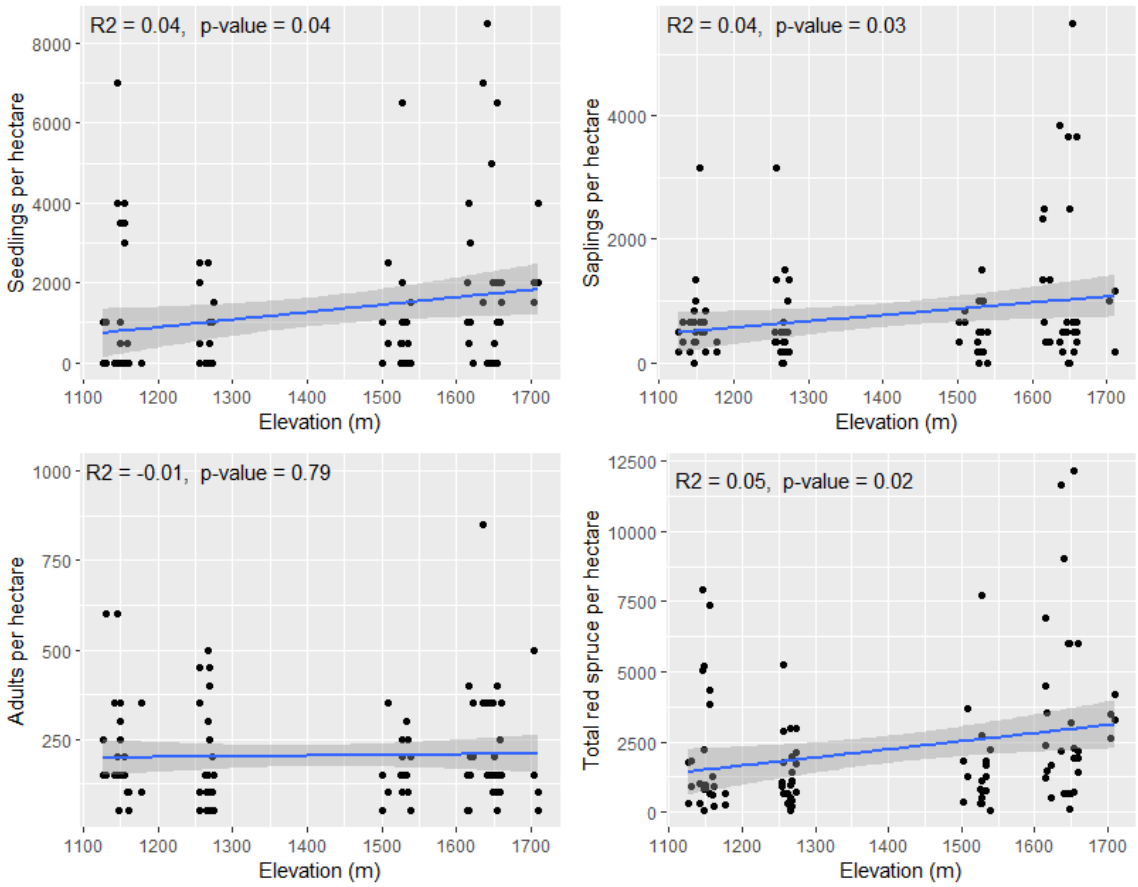

Figure 19 Correlations between elevation in meters and seedling counts, sapling counts, adult counts, and sum counts across cohorts.

Climate Models:

All climate change scenarios for the 2021 – 2040 period showed a dramatic decrease in suitable habitat with shared socioeconomic pathway 126 (SSP126 = < 2°C warming by 2100) maintaining the most suitable habitat, shared socioeconomic pathway 370 (SSP370 = < 4°C warming by 2100) having the least suitable habitat, and shared socioeconomic pathway 245 (SSP245 = < 3°C warming by 2100) having an intermediate amount of suitable habitat (Table 7). The only remaining suitable habitat by 2040 in all three scenarios was contained to the Mount Rogers area representing the highest elevations in Virginia (Figure 20). A 98.095%, 98.699%, and 99.899% decrease from

current suitable habitat occurred in the SSP126, SSP245, and SSP370 scenarios respectively (Table 8). Maximum temperatures of the warmest month at recorded presence points increased substantially across all scenarios. SSP126 had the smallest increase in temperatures followed by SSP245 then SSP370. May precipitation amounts decreased from their current amounts across all scenarios with greater and nearly equal decreases between SSP245 and SSP370 (Figure 21).

Table 7 Comparison of area (in hectares) occupied by each probability bin for shared socioeconomic pathway 126 (SSP126), shared socioeconomic pathway 245 (SSP245), and shared socioeconomic pathway 370 (SSP370).

Probability Bin	SSP126 (ha)	SSP245 (ha)	SSP370 (ha)
0.0 – 0.2	11060087.49	11060987.49	11062004.58
0.2 – 0.4	208.53	256.59	82.44
0.4 – 0.6	188.01	98.01	47.97
0.6 – 0.8	277.74	233.55	88.92
0.8 – 1.0	1559.88	743.85	97.74

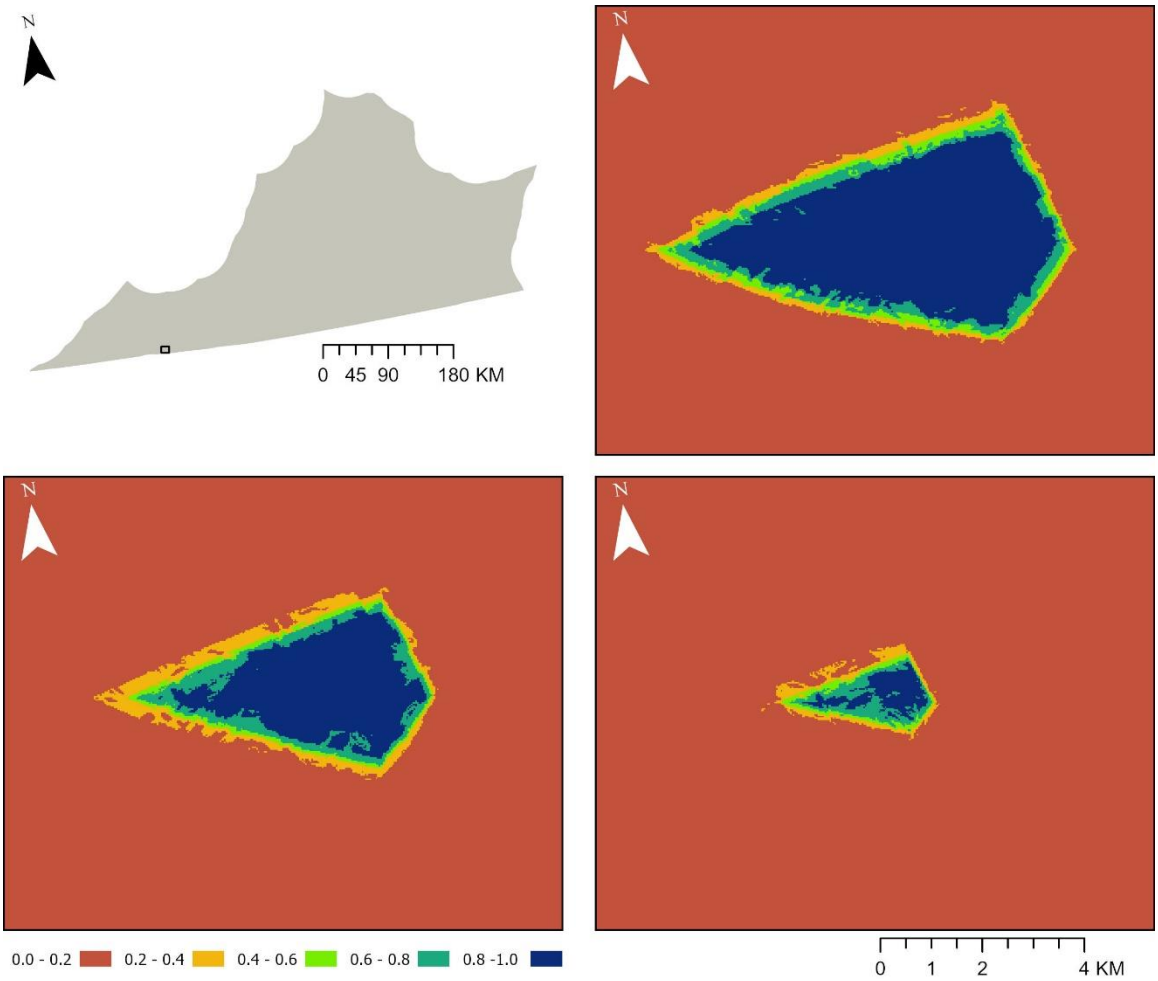

Figure 20 Visual comparison of red spruce suitable habitat by 2040 in shared socioeconomic pathway 126 (SSP126; top right), shared socioeconomic pathway 245 (SSP245; bottom left), and shared socioeconomic pathway 370 (SSP370; bottom right).

Table 8 Changes in suitable habitat by 2040 given shared socioeconomic pathway 126 (SSP126), shared socioeconomic pathway 245 (SSP245), and shared socioeconomic pathway 370 (SSP370).

Scenario	Loss (%)	Gain (%)	Net Loss (%)
SSP126	98.439	0.344	98.095
SSP245	98.741	0.042	98.699
SSP370	99.899	0	99.899

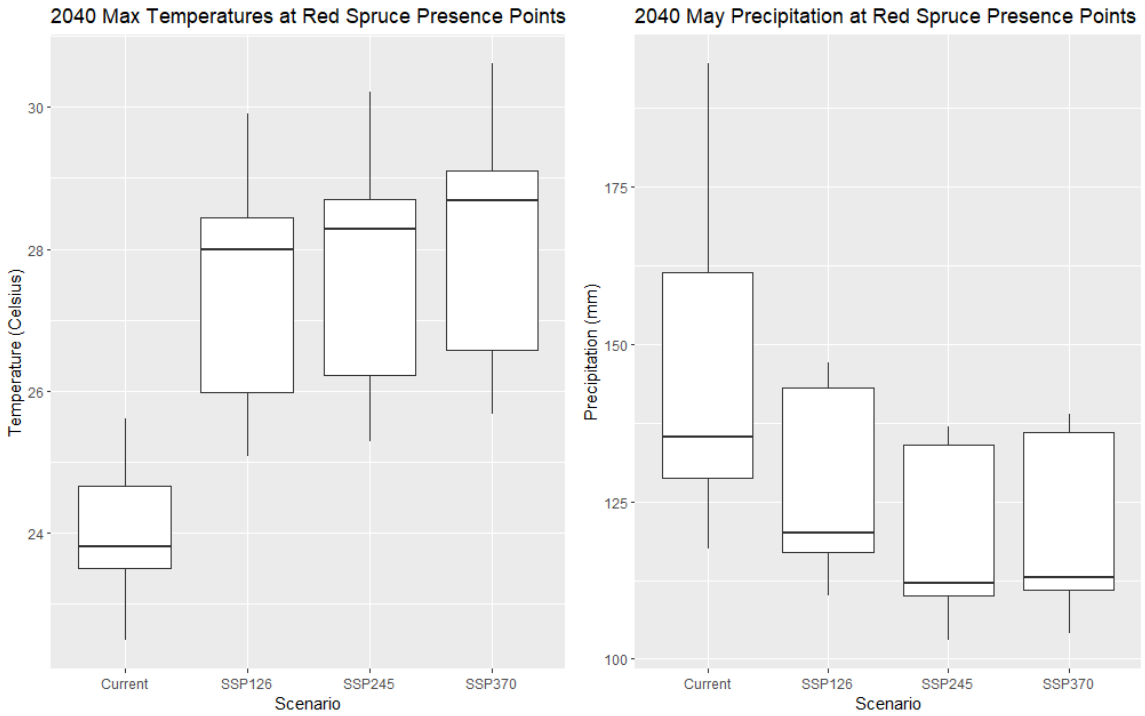

Figure 21 2040 Maximum temperatures of the warmest month currently and across given shared socioeconomic pathway 126 (SSP126), shared socioeconomic pathway 245 (SSP245), and shared socioeconomic pathway 370 (SSP370) (left) and May Precipitation currently and across SSP126, SSP245, and SSP370 (right).

By 2100, all climate change scenarios predicted an elimination of red spruce suitable habitat from Virginia (Table 9). Remarkably, the 2100 median maximum temperature of the warmest month in the SSP370 scenario surpasses 33°C at recorded red spruce occurrences. 2100 May precipitation amounts showed a similar pattern in decline as 2040 May precipitation, however, precipitation amounts are higher by 2100 compared to 2040 (Figure 21; Figure 22).

Table 9 Comparison of area (in hectares) occupied by each probability bin for shared socioeconomic pathway 126 (SSP126), shared socioeconomic pathway 245 (SSP245), and shared socioeconomic pathway 370 (SSP370).

Probability Bin	SSP126 (ha)	SSP245 (ha)	SSP370 (ha)
0.0 – 0.2	11417057.01	11417057.01	11417057.01
0.2 – 0.4	0	0	0
0.4 – 0.6	0	0	0
0.6 – 0.8	0	0	0
0.8 – 1.0	0	0	0

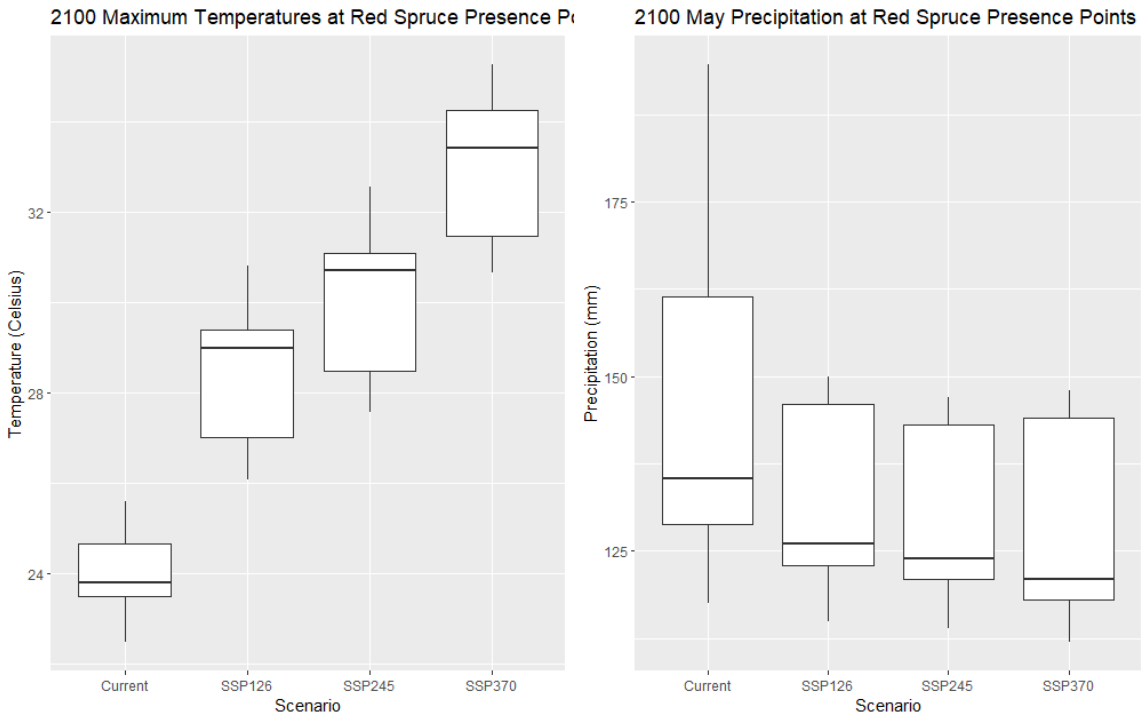

Figure 22 2100 Maximum temperatures of the warmest month currently and across given shared socioeconomic pathway 126 (SSP126), shared socioeconomic pathway 245 (SSP245), and shared socioeconomic pathway 370 (SSP370) (left) and May Precipitation currently and across SSP126, SSP245, and SSP 370 (right).

DISCUSSION

This study elucidated the current restoration potential of red spruce and investigated how this potential may be altered by predicted climate change over the course of the 21st century. Current distribution and potential red spruce distribution were modeled separately to define the spatial extent to which red spruce can expand into. Forest surveys were conducted to assess the current state of red spruce regeneration. Ecological niche models (ENMs) were also used to project how mild and severe climate change scenarios would affect the habitat suitability of red spruce. Results indicate that red spruce has unoccupied suitable habitat available to expand into and is actively expanding into these spaces adjacent to existing red spruce stands. However, climate

change will likely have a strong, indirect negative effect on red spruce, regardless of the climate scenario.

As predicted, suitable habitat was greater than the current distribution of red spruce, as indicated by species distribution model (SDM) and habitat suitability model (HSM) area comparisons (Figure 13). The trend of suitable habitat being greater than current distribution was generally true across all sites in Virginia. The contrast in distribution and habitat suitability is more than likely due to arrested regeneration as a results of acute anthropogenic disturbance events since the late 1800's (Pielke 1981, Blum 1990, Griscom and Griscom 2011, Hamburg and Cogbill 1984, Bliss and Vogelmann 1982). Consequently, it can be concluded that, in a spatial context, red spruce has a high restoration potential.

The forest surveys conducted to assess the regeneration patterns of red spruce in Virginia showed no significant differences between sites in terms of red spruce counts, with the exception of marginal significance in the seedling cohort (Figure 15). General patterns are, however, evident in the data. The Southern Appalachian sites at Mount Rogers (MTR; median = 275) and Whitetop Mountain (WTP; median = 400) generally had higher counts across all cohorts when compared to the Central Appalachian sites at the Highland County grassy bald (HCGB; median = 167) and Highland County stand (HCSD; median = 275). The WTP site had exceptionally high regeneration compared to other sites. Unique to WTP plots was a strong dominance by red spruce, with very few other tree species present in a large portion of plots. Therefore the high regeneration observed at WTP can most likely be ascribed to a dearth of competition for red spruce at this site. In contrast, MTR red spruce faced strong competition from balsam fir (*Abies*

balsamea) and fraser fir (*Abies fraseri*). HCGB and HCSD red spruce likewise existed in much more mixed stands with greater abundance of associated species such as yellow birch (*Betula alleghaniensis*), red maple (*Acer rubrum),* and Canadian hemlock (*Tsuga canadensis*).

Forest surveys also showed that red spruce is expanding into the additional unoccupied suitable habitat available to it (Table 6).As would be expected, red spruce seedling and sapling counts were generally higher in the interior (median = 667 seedlings and saplings per hectare) than in the exterior (median = 500 seedlings and saplings per hectare) of red spruce canopies (Figure 16). However, regeneration was shown to be occurring in the exterior of canopies. Further, red spruce is advancing in life stage as frequently in the exterior as within the interior of the stand (Figure 18). Such strong regeneration patterns are likely due to a number of relatively recent environmental shifts. The reduction of acid deposition in soils due to air pollution, as well as increases in atmospheric CO2 and temperature are the most likely explanatory variables for the observed regeneration trends (Mathias and Thomas 2018, Li et al. 2020). While current models and regeneration trends indicate positive regeneration, climate projections predict a difficult future for red spruce.

A mild climate change scenario (< 2°C warming) socio-economic pathway 126 (SSP126), an intermediate climate change scenario (< 3°C warming) socioeconomic pathway 245 (SSP245), and a severe climate change scenario (< 4°C warming) socio-economic pathway 370 (SSP370) were used to project how red spruce suitable habitat will be affected by climate change. In all three scenarios red spruce suitable habitat was diminished to near zero by 2040 and completely eliminated by 2100 (Table 7; Table 9).

However, the predicted elimination of suitable habitat is not the same as the extirpation of current red spruce stands in Virginia. Understanding HSM predictions and by extension climate model predictions is necessary to draw accurate conclusions about the future of red spruce in Virginia.

In this study the HSM used as the basis for climate projections exhibited a sharp decline in the probability of the occurrence of suitable red spruce habitat at 26°C in the maximum temperature of the warmest month (MxTpWrmMth) variable, as indicated by response curves (Figure 10). The absence of suitable habitat beyond a maximum temperature of 26°C is contrary to known physiological limitations of red spruce. In terms of maximum temperatures, red spruce becomes severely limited in its ability to regenerate around 33°C, as the seed viability is compromised at this temperature. However, recent studies have consistently shown adult red spruce growth to respond positively to increases in temperature, with stronger responses at the colder extents of its distribution, indicating cold-stress as an important limiting factor as opposed to heat-stress (Mathias and Thomas 2018, Li et al. 2020). Furthermore, in this study red spruce regeneration quantified in field surveys was not found to be positively or negatively correlated with elevation, a strong correlate of temperature, indicating there is no evidence for temperature related physiological limits in Virginia populations at either elevational extent of the red spruce distribution (Figure 19). Because there is no evidence of abiotic environmental limitations present for red spruce in Virginia, the most likely alternative explanation for the 26°C maximum temperature threshold is biotic interactions.

Murphy (1917) noted that red spruce occurred in the habitat that it did, not because it was particularly well adapted to it, rather because most other species were poorly adapted to that habitat. Many tree species common to the lower elevations of the Appalachians like pines (*Pinus spp.*) and oaks (*Quercus spp.*) are poorly adapted to the relatively small number of growing degree days, shallow and acidic soils, or intense moisture found in red spruce habitat (Davis et al. 2017). When compared to balsam fir, a species adapted to the cool and moist environments of the Appalachian Mountains, red spruce is outcompeted on a physiological basis (Dumais and Prevost 2008). Therefore the 26°C threshold likely represents the point at which red spruce can be outcompeted by low elevation tree species, rather than a physiological limitation inherent to red spruce in responses to the abiotic environment. While the HSM provides data useful for elucidating the limitations of red spruce habitat at lower elevations, the unique approach of modeling distribution separately in the SDM allows further inferences to be made regarding the limitations of red spruce at its upper elevational extent.

A novel approach in ecological niche modeling was taken in which models were manipulated to predict current distribution (SDM) and potential distribution (HSM) separately, providing additional insight into the ecological challenges faced by red spruce. The inclusion of true absence points located in close proximity to presence points in the distribution model successfully caused a greater discrimination to occur in the SDM when compared to the HSM. The resulting SDM was able to identify more nuanced relationships between presence points and their environment when compared with the HSM. For example, the SDM was able to detect a decline in the probability of occurrence at temperatures below approximately 23°C whereas the HSM response curves did not

portray this decline (Figure 6 and Figure 10). This decline at the lower extent of the maximum temperatures of the warmest month (MxTpWrmMth) likely reflects an increase in competition for red spruce at the colder extremes. Cold-adapted tree species such as balsam fir and fraser fir provide competition for red spruce at elevations where few other species can thrive (Dumais and Prevost 2008). An alternative, but not mutually exclusive explanation for the decline in the probability of occurrence at the lowest maximum temperatures could be cold stress. This alternative explanation is much less likely as red spruce has been found to exist in environments with maximum temperatures of just 21°C while decline in probability of occurrence begins as maximum temperatures decrease below 23°C (Blum 1990, Figure 6).

Interestingly, SDMs had noticeably lower true skill statistic (TSS) and area under the receiver operating characteristic curve (ROC) scores than those of the HSMs (Figure 5; Figure 9). Such high evaluation scores in the HSM can indicate that overfitting occurred in some cases of individual models. Overfitting occurs when models perfectly fit to the training data, which greatly inhibits a model's ability to extend accurate predictions to data which is not included in the training dataset. In this study, the influence of the few overfitted models were limited by ensemble averaging with normally fitted models. Although SDMs had lower evaluation scores when compared to HSMs, SDMs clearly had greater discriminatory ability (Figure 5; Figure 9; Figure 14). Therefore the lower SDM scores more likely reflect the difficulty of the modeling objective as opposed to poor performance in achieving that modeling objective. SDMs regularly encountered data which was contradictory (e.g. presence and absence points with the same environmental variable values) on a non-random basis due to the use of

true-absence points in proximity to presence points, making distribution more difficult to model. In contrast, HSMs only dealt with randomly generated pseudo-absence points in which contradictory data points occurred on a purely random basis and therefore carried less weight in models. While modeling distribution separately from habitat suitability was demonstrated to be a useful method in this study, the novelty of this technique leaves much to be explored in terms of its implementation.

A question that remains about implementing true absence points in close proximity to presence points to model distribution is whether this method can be used for species with broad niches. Because red spruce has such a narrow niche, it is relatively easy to collect points at the edges of its distribution. However, such sampling with a wide-spread species would be considerably more difficult and would likely take many more absence points to produce a meaningful change in model outcomes. There is also the possibility of incorporating an environmental variable in models which describes the limitations of a species distribution in lieu of absence points to produce a distribution model, rather than a suitability model. Chen and Leites (2020) implemented an environmental variable which accounted for land use legacies when modeling species distributions. This method could be used to differentiate between distributions and habitat suitability for species which have experienced anthropogenic disturbances from which they have not yet recovered.

It was predicted that MxTpWrmMth and average annual precipitation would be the most important variables for modeling red spruce distribution and habitat. As expected, MxTpWrmMth was the most important variable, most likely due to temperature mediated effects on red spruce competition. Contrary to predictions, average

precipitation in May (MayPrecip) was another important variable instead of average annual precipitation. This may be explained by the timing of red spruce germination which occurs in May (Blum 1990). Moisture levels are known to be the primary determinant of germination and MayPrecip therefore plays a primary role in determining the distribution and habitat suitability of red spruce. While less important relative to MxTpWrmMth and MayPrecip, total insolation derived from direct and diffuse, but not reflected, radiation for the summer solstice (radsumsol) played a significant role in identifying distribution and suitable habitat at smaller scales. Of particular importance to the models was that radsumsol enabled models to discriminate between north and south facing slopes. North facing slopes are cooler and have greater moisture levels, making them more suitable to red spruce when compared to the hotter and drier south facing slopes. Geological variables were the most distal variables considered for use in models due to the variables being defined in terms of distance rather than presence or absence of a geological parent material. Further complicating the choice of geological variable is the geological diversity of the Blue Ridge and Ridge and Valley regions in Virginia. Despite being the most important variable amongst the geological category, distance to acidic shale bedrock (geo200) had very little impact on modeling outcomes with response curves commonly disagreeing, both within and between algorithm types (Figure 6; Figure 10).

CONCLUSION

In the present, red spruce has a strong restoration potential in Virginia, with natural regeneration occurring in the Central and Southern Appalachian Mountains in both the interior and exterior of spruce canopies. However, competition is likely to

increase for red spruce as a result of climate change over the course of the 21st century. Therefore, restoration management in Virginia should be aimed at 1) increasing existing red spruce stands resistance to competition and 2) planting red spruce in areas where competition is least likely in the future.

The primary priority of land managers in terms of increasing red spruce resistance to competition should be protecting and expanding the existing mature stands of red spruce. Not only are mature stands more resistant to competition due to their establishment, but the environment beneath the canopy of a red spruce stand is conducive to red spruce germination and growth and even counterproductive to the germination of species which prefer high light levels and are intolerant of highly saturated substrates. Because red spruce is slow growing and takes many years to reach reproductive maturity, it is likely to be outcompeted by most species in the short term. Less mature and more mixed red spruce stands at lower elevations will therefore likely see a shift in representation to faster growing hardwood tree species, such as red maple (*Acer rubrum*), striped maple (*Acer pensylvanicum*), and Fraser magnolia (*Magnolia fraseri*). However, red spruce stands in environments which are disadvantageous to the recruitment of low-elevation species are likely to see the least amount of change in species composition. Therefore, protecting mature red spruce stands limits competition and maintains regeneration. Should climate conditions return to their pre-industrial levels, red spruce would likely continue with the strong regeneration trends observed over the last two decades; however, the rate at which this regeneration occurs is strongly dependent on the number and maturity of stands remaining by the time conditions are ameliorated.

Several high elevation species in Virginia which might otherwise outcompete red spruce are declining due to insect infestations opening a niche for red spruce. Fraser fir (*Abies fraseri*) and balsam fir, as well as Canadian hemlock (*Tsuga canadensis*) have been greatly damaged in Virginia due to the balsam wooly adelgid (*Adeleges piceae*) and the hemlock wooly adelgid (*Adelges tsugae*) respectively (McManamay et al 2011, Spaulding and Rieske 2010). The primary pest of red spruce, the spruce budworm (*Choristoneura fumiferana*) only affects populations in the Northern Appalachians and to a minimal degree at that (Seymour 1992). With the reduction of these high elevation species, additional habitat for red spruce to may open where competition from low elevation species will be less intense. It may therefore be advantageous to plant red spruce in these high elevation areas in preparation for the expected ecological shifts due to climate change and pest infestations to establish a head start for red spruce.

APPENDIX A

Table A1 93 environmental variables provided Virginia Department of Conservation and Recreation Division of Natural Heritage, classified as proximal or distal.

Variable	Category	Description	Classification
elevx10	Elevation and Derivatives	Elevation in centimeters (originally in meters)	Distal
slopex100	Elevation and Derivatives	The inclination of slope in degrees.	Distal
crvslpx100	Elevation and Derivatives	The curvature of a cell as fitted through that cell and its neighbors.	Distal
crvprox100	Elevation and Derivatives	The curvature of a cell in the direction of the maximum slope. Affects the acceleration and deceleration of flow and, therefore, influences erosion and deposition	Distal
crvplax100	Elevation and Derivatives	The curvature of a cell perpendicular to the direction of the maximum slope. Influences convergence and divergence of flow	Distal
radsumsol	Elevation and Derivatives	Total insolation derived from direct and diffuse, but not reflected, radiation for the summer solstice	Proximal
radequinx	Elevation and Derivatives	Total insolation derived from direct and diffuse, but not reflected, radiation for the equinox	Proximal
radwinsol	Elevation and Derivatives	Total insolation derived from direct and diffuse, but not reflected, radiation for the winter solstice	Proximal
rgh1cx100	Elevation and Derivatives	The standard deviation of elevation values within the neighborhood immediately surrounding the center cell.	Distal
rgh10cx100	Elevation and Derivatives	The standard deviation of elevation values within a circular neighborhood with a radius of 10 cells.	Distal
rgh100x100	Elevation and Derivatives	The standard deviation of elevation values within a circular neighborhood with a radius of 100 cells.	Distal
beersx1000	Elevation and Derivatives	Beers et al. (1966) transformation of slope direction. Original scale is 0 (SW, most exposed) to 2 (NE, most sheltered), with values grading equivalently in both directions between the extremes.	Distal
distinlwat	Hydrography	Euclidean distance to nearest stream, river, or other inland waterbody (excluding estuaries)	Distal
diststrm	Hydrography	Euclidean distance to nearest stream (features represented by lines only)	Distal
distcstwat	Hydrography	Euclidean distance to nearest estuary or sea/ocean. [This probably can be tossed since only differs from estuaries if youÃ¯Â¿Â½re in the middle of the ocean or on an island with no estuaries identified]	Distal
distocean	Hydrography	Euclidean distance to nearest sea/ocean	Distal
distestury	Hydrography	Euclidean distance to nearest estuary	Distal
downdist	Hydrography	The downslope distance along the flow path to a water or wetland feature.	Distal
flowacc	Hydrography	Flow accumulation is used as a proxy for topographic moisture. For each cell, this is determined by summing the weights of all cells flowing into it. This does not account for flow differences over different soil types.	Distal

Variable	Category	Description	Classification
canopy1	Land cover - NLCD	mean percent canopy cover in 1-cell radius (30 meter cells)	Distal
canopy10	Land cover - NLCD	mean percent canopy cover in 10-cell radius (30 meter cells)	Distal
canopy100	Land cover - NLCD	mean percent canopy cover in 100-cell radius (30 meter cells)	Distal
impsur1	Land cover - NLCD	mean percent impervious cover in 1-cell radius (30 meter cells)	Distal
impsur10	Land cover - NLCD	mean percent impervious cover in 10-cell radius (30 meter cells)	Distal
impsur100	Land cover - NLCD	mean percent impervious cover in 100-cell radius (30 meter cells)	Distal
nlcdopn1	Land cover - NLCD	mean open cover within 1-cell radius	Distal
nlcdopn10	Land cover - NLCD	mean open cover within 10-cell radius	Distal
nlcdopn100	Land cover - NLCD	mean open cover within 100 cell radius	Distal
nlcdshb1	Land cover - NLCD	mean shrub cover within 1-cell radius	Distal
nlcdshb10	Land cover - NLCD	mean shrub cover within 10-cell radius	Distal
nlcdshb100	Land cover - NLCD	mean shrub cover within 100 cell radius	Distal
nlcdwat1	Land cover - NLCD	mean open water cover within 1-cell radius	Distal
nlcdwat10	Land cover - NLCD	mean open water cover within 10-cell radius	Distal
nlcdwat100	Land cover - NLCD	mean open water cover within 100 cell radius	Distal
nlcdwet1	Land cover - NLCD	mean wetland cover within 1-cell radius	Distal
nlcdwet10	Land cover - NLCD	mean wetland cover within 10-cell radius	Distal
nlcdwet100	Land cover - NLCD	mean wetland cover within 100 cell radius	Distal
dnwiffw	Land cover - NWI	Distance to forested palustrine wetland	Distal
dnwifemw	Land cover - NWI	Distance to freshwater emergent wetland	Distal
dnwisemw	Land cover - NWI	Distance to saltwater emergent wetland	Distal
gddays	Climate: temperature	Growing degree days	Proximal
geo001	Geology (distance to types)	Euclidean distance to sand	Distal
geo002	Geology (distance to types)	Euclidean distance to loam	Distal
geo003	Geology (distance to types)	Euclidean distance to silt/clay	Distal
geo031	Geology (distance to types)	Euclidean distance to coastal plain sand over limestone	Distal
geo032	Geology (distance to types)	Euclidean distance to coastal plain loam over limestone	Distal

Variable	Category	Description	Classification
geo033	Geology (distance to types)	Euclidean distance to coastal plain silt and clay over limestone	Distal
geo100	Geology (distance to types)	Euclidean distance to acidic sedimentary bedrock	Proximal
geo200	Geology (distance to types)	Euclidean distance to acidic shale bedrock	Proximal
geo300	Geology (distance to types)	Euclidean distance to calcareous bedrock	Proximal
geo400	Geology (distance to types)	Euclidean distance to moderately calcareous bedrock	Proximal
geo500	Geology (distance to types)	Euclidean distance to acidic granitic bedrock	Proximal
geo600	Geology (distance to types)	Euclidean distance to mafic bedrock	Proximal
geo700	Geology (distance to types)	Euclidean distance to ultramafic bedrock	Proximal
JulyPrecip	Climate: precipitation	July precipitation	Proximal
JunePrecip	Climate: precipitation	June precipiation	Proximal
MayPrecip	Climate: precipitation	May precipitation	Proximal
NrmDspPrcp	Climate: precipitation	normalized dispersion (CV) of precipitation	Proximal
PrcpCldQtr	Climate: precipitation	precipitation of coldest quarter	Proximal
PrcpDryMth	Climate: precipitation	precipitation of driest month	Proximal
PrcpDryQtr	Climate: precipitation	precipitation of driest quarter	Proximal
PrcpWrmQtr	Climate: precipitation	precipitation of warmest quarter	Proximal
PrcpWetMth	Climate: precipitation	precipitation of wettest month	Proximal
PrcpWetQtr	Climate: precipitation	precipitation of wettest quarter	Proximal
TtlAnnPrcp	Climate: precipitation	total annual precipitation	Proximal
AnnMnTemp	Climate: temperature	annual mean temperature	Proximal
Isotherm	Climate: temperature	comparison of day-to-night and summer-to-winter temperature oscillations	Proximal
MxTpWrmMth	Climate: temperature	maximum temperature of warmest month	Proximal
MnDiurnRng	Climate: temperature	(mean of monthly (max temp - min temp))	Proximal
MnTpCldQtr	Climate: temperature	mean temperature of coldest quarter	Proximal
MnTpDryQtr	Climate: temperature	mean temperature of driest quarter	Proximal
MnTpWrmQtr	Climate: temperature	mean temperature of warmest quarter	Proximal

Variable	Category	Description	Classification
MnTpWetQtr	Climate: temperature	mean temperature of wettest quarter	Proximal
MnTpCldMth	Climate: temperature	minimum temperature of coldest month	Proximal
TempAnnRng	Climate: temperature	(max temp warmest month - min temp coldest month)	Proximal
TempSeason	Climate: temperature	(STD * 100)	Proximal
distriver	Hydrography	Euclidean distance to nearest stream/river	Distal
distpond	Hydrography	Euclidean distance to nearest lake/pond/resevoir <= 1 ha	Distal
distlake	Hydrography	Euclidean distance to nearest lake/pond/resevoir > 1 ha	Distal
tp001x1000	Elevation and Derivatives	Topographic position index using elevation values within the neighborhood immediately surrounding the center cell	Distal
tp010x1000	Elevation and Derivatives	Topographic position index using elevation values within a circular neighborhood with a radius of 10 cells.	Distal
tp100x1000	Elevation and Derivatives	Topographic position index using elevation values within a circular neighborhood with a radius of 100 cells.	Distal
nlcddfr1	Land cover - NLCD	mean deciduous forest cover within 1-cell radius	Distal
nlcddfr10	Land cover - NLCD	mean deciduous forest cover within 10-cell radius	Distal
nlcddfr100	Land cover - NLCD	mean deciduous forest cover within 100-cell radius	Distal
nlcdefr1	Land cover - NLCD	mean evergreen forest cover within 1-cell radius	Distal
nlcdefr10	Land cover - NLCD	mean evergreen forest cover within 10-cell radius	Distal
nlcdefr100	Land cover - NLCD	mean evergreen forest cover within 100-cell radius	Distal
radswdiff	Elevation and Derivatives	Difference between Summer and Winter solstice total insolation derived from direct and diffuse, but not reflected, radiation [radsumsol - radwinsol]	Proximal
distsink	Karst features	Euclidean distance to sinkholes	Distal
denssink	Karst features	Kernel density of sinkholes	Distal
latx10k	Map-based information	The latitudinal values	Distal
distkarst	Karst features	Euclidean distance to karst features in the Ridge and Valley Region	Distal

Table A2 Raw importance values for each proximal enviromental variable. Importance calculations were carried out within variable categories. *GLM importance values were ignored in the Climate: temperature and Geology (distance to types) categories when calculating averages due to a majority of variables being excluded from GLM equations; The highest average values of each category are highlighted.

Category	Variable	*GLM	GBM	RF	GAM	Average
Elevation and Derivatives	radsumsol	1.00	1.00	0.94	1.00	0.99
	radequinx	0.74	0.07	0.20	0.75	0.44
	radwinsol	1.00	0.34	0.40	1.00	0.69
Geology (distance to types)	geo100	0.00	0.01	0.01	0.30	0.11
	geo200	1.00	0.19	0.07	0.64	0.30
	geo300	0.31	0.02	0.04	0.44	0.17
	geo400	0.00	0.02	0.05	0.57	0.21
	geo500	0.38	0.00	0.02	0.59	0.20
	geo600	0.00	0.02	0.03	0.63	0.23
	geo700	0.58	0.01	0.02	0.58	0.20
Climate: Precipitation	JulyPrecip	0.07	0.00	0.01	0.59	0.17
	JunePrecip	0.06	0.07	0.07	0.61	0.20
	MayPrecip	0.89	0.34	0.13	0.89	0.56
	NrmDspPrcp	0.62	0.02	0.03	0.55	0.31
	PcrcpCldQtr	0.22	0.01	0.01	0.59	0.21
	PrcpDryMth	0.09	0.05	0.06	0.57	0.19
	PrcpDryQtr	0.75	0.15	0.13	0.78	0.45
	PrcpWrmQtr	0.05	0.00	0.01	0.69	0.19
	PrcpWetMth	0.30	0.00	0.01	0.69	0.25
	PrcpWetQtr	0.44	0.00	0.01	0.68	0.28
	TtlAnnPrcp	1.00	0.05	0.08	0.65	0.45
Climate: Temperature	gddays	0.00	0.00	0.02	0.52	0.18
	AnnMnTemp	0.93	0.01	0.02	0.52	0.18
	Isotherm	0.13	0.00	0.02	0.60	0.21
	MxTpWrmMth	0.00	0.10	0.06	0.73	0.30
	MnDiurnRng	0.00	0.02	0.03	0.84	0.30
	MnTpCldQtr	0.00	0.03	0.02	0.75	0.27
	MnTpDryQtr	0.00	0.00	0.01	0.58	0.20
	MnTpWrmQtr	0.00	0.08	0.06	0.60	0.25
	MnTpWetQtr	0.03	0.00	0.02	0.49	0.17
	MnTpCldMth	0.00	0.00	0.01	0.73	0.25
	TempAnnRng	0.00	0.00	0.02	0.78	0.27
	TempSeason	0.00	0.07	0.02	0.59	0.23

Table A3 Individual species distribution model (SDM) scores including model ID (algorithm type, run number, psuedo-absence sample), evaluation metrics, testing data (overall model perfomance), cutoff (integerized threshold for binary map construction), sensitivity, and specificity

Model ID	Evaluation Metric	Testing Data	Cutoff	Sensitivity	Specificity
GLMRun1PA1	KAPPA	0.601	495	92.647	78.5
	TSS	0.711	495	92.647	78.5
	ROC	0.856	500	92.647	78.5
GAMRun1PA1	KAPPA	0.763	777	98.529	87
	TSS	0.855	777	98.529	87
	ROC	0.949	720.5	100	86
RFRun1PA1	KAPPA	0.809	626	89.706	93.5
	TSS	0.850	328	98.529	86.5
	ROC	0.975	332	98.529	86.5
GBMRun1PA1	KAPPA	0.810	835	91.176	93
	TSS	0.846	786	94.118	90.5
	ROC	0.964	794.5	94.118	91.
GLMRun2PA1	KAPPA	0.852	307	98.529	92.5
	TSS	0.910	307	98.529	92.5
	ROC	0.975	310	98.529	92.5
GAMRun2PA1	KAPPA	0.860	267	97.059	93.5
	TSS	0.906	267	97.059	93.5
	ROC	0.977	270	97.059	93.5
RFRun2PA1	KAPPA	0.884	278	94.118	96
	TSS	0.901	278	94.118	96
	ROC	0.985	280	94.118	96
GBMRun2PA1	KAPPA	0.883	464	92.647	96.5
	TSS	0.905	55	100	90.5
	ROC	0.983	58	100	90.5
GLMRun3PA1	KAPPA	0.763	372	98.529	87
	TSS	0.855	372	98.529	87
	ROC	0.950	371.5	98.529	87
GAMRun3PA1	KAPPA	0.756	605	94.118	88.5
	TSS	0.855	91	100	85.5
	ROC	0.961	91.5	100	85.5
RFRun3PA1	KAPPA	0.821	500	85.294	96
	TSS	0.866	303	95.588	91
	ROC	0.980	304	95.588	91
GBMRun3PA1	KAPPA	0.832	738	86.765	96
	TSS	0.852	639	91.176	94
	ROC	0.980	639.5	91.176	94
GLMRun1PA2	KAPPA	0.698	495	100	82
	TSS	0.820	495	100	82
	ROC	0.910	500	100	82

Model ID	Evaluation Metric	Testing Data	Cutoff	Sensitivity	Specificity
GAMRun1PA2	KAPPA	0.793	787	91.176	92
	TSS	0.856	505	97.059	88
	ROC	0.954	510.5	97.059	89
RFRun1PA2	KAPPA	0.867	394	95.588	94
	TSS	0.906	379	97.059	93.5
	ROC	0.978	380	97.059	93.5
GBMRun1PA2	KAPPA	0.860	606.5	97.059	93.5
	TSS	0.906	606.5	97.059	93.5
	ROC	0.972	606	97.059	93.5
GLMRun2PA2	KAPPA	0.776	673	97.059	88.5
	TSS	0.856	673	97.059	88.5
	ROC	0.961	678	97.059	88.5
GAMRun2PA2	KAPPA	0.740	499	98.529	85.5
	TSS	0.840	499	98.529	85.5
	ROC	0.950	503.5	98.529	85.5
RFRun2PA2	KAPPA	0.831	465	94.118	93
	TSS	0.871	465	94.118	93
	ROC	0.973	468	94.118	93
GBMRun2PA2	KAPPA	0.805	631	94.118	91.5
	TSS	0.870	281	100	87
	ROC	0.974	295	100	87.5
GLMRun3PA2	KAPPA	0.705	495	100	82.5
	TSS	0.825	495	100	82.5
	ROC	0.912	500	100	82.5
GAMRun3PA2	KAPPA	0.776	449	97.059	88.5
	TSS	0.856	449	97.059	88.5
	ROC	0.952	446.5	97.059	88.5
RFRun3PA2	KAPPA	0.851	500	88.235	96.5
	TSS	0.847	500	88.235	96.5
	ROC	0.978	503	88.235	96.5
GBMRun3PA2	KAPPA	0.826	770	89.706	94.5
	TSS	0.855	60	100	85.5
	ROC	0.979	61	100	85.5
GLMRun1PA3	KAPPA	0.620	495	79.412	86.5
	TSS	0.659	495	79.412	86.5
	ROC	0.830	500	79.412	86.5
GAMRun1PA3	KAPPA	0.788	544	100	88
	TSS	0.880	544	100	88
	ROC	0.959	545	100	88
RFRun1PA3	KAPPA	0.892	459	92.647	97
	TSS	0.901	318	97.059	93
	ROC	0.987	318	97.059	93
GBMRun1PA3	KAPPA	0.867	613	95.588	94.5
	TSS	0.901	613	95.588	94.5

Model ID	Evaluation Metric	Testing Data	Cutoff	Sensitivity	Specificity
	ROC	0.987	612.5	95.88	94.5
GLMRun2PA3	KAPPA	0.705	553	100	82.5
	TSS	0.825	553	100	82.5
	ROC	0.916	554	100	82.5
GAMRun2PA3	KAPPA	0.797	685	94.118	90.5
	TSS	0.851	685	94.118	90.5
	ROC	0.972	688.5	94.118	91
RFRun2PA3	KAPPA	0.858	606	85.294	98
	TSS	0.881	303	95.588	92.5
	ROC	0.985	301	95.588	92.5
GBMRun2PA3	KAPPA	0.866	616.5	94.118	95
	TSS	0.891	616.5	94.118	95
	ROC	0.981	618	94.118	95
GLMRun3PA3	KAPPA	0.705	495	95.588	84.5
	TSS	0.801	495	95.588	84.5
	ROC	0.900	495	95.588	84.5
GAMRun3PA3	KAPPA	0.810	763	91.176	93
	TSS	0.866	515	97.059	89.5
	ROC	0.965	520	97.059	90
RFRun3PA3	KAPPA	0.885	470	95.588	95.5
	TSS	0.911	470	95.588	95.5
	ROC	0.986	468	95.588	95.5
GBMRun3PA3	KAPPA	0.874	776	92.647	96
	TSS	0.896	662	95.588	94
	ROC	0.984	662.5	95.588	94

Table A4 Individual habitat suitability model (HSM) scores including model ID (algorithm type, run number, psuedo-absence sample), evaluation metrics, testing data (overall model perfomance), cutoff (integerized threshold for binary map construction), sensitivity, and specificity.

Model ID	Evaluation Metric	Testing Data	Cutoff	Sensitivity	Specificity
GLMRun1PA1	KAPPA	0.971	434	100	98.5
	TSS	0.985	434	100	98.5
	ROC	0.992	436.5	100	98.5
GAMRun1PA1	KAPPA	0.971	359	98.529	99
	TSS	0.975	359	98.529	99
	ROC	0.988	360.5	98.529	99
RFRun1PA1	KAPPA	0.990	697	100	99.5
	TSS	0.995	697	100	99.5
	ROC	1.000	696	100	99.5
GBMRun1PA1	KAPPA	0.971	338	100	98.5
	TSS	0.985	338	100	98.5
	ROC	0.997	343	100	98.5
GLMRun2PA1	KAPPA	1.000	934	100	100
	TSS	1.000	934	100	100
	ROC	1.000	935	100	100
GAMRun2PA1	KAPPA	0.980	495	97.059	100
	TSS	0.971	495	97.059	100
	ROC	0.985	500	97.059	100
RFRun2PA1	KAPPA	1.000	556	100	100
	TSS	1.000	556	100	100
	ROC	1.000	555	100	100
GBMRun2PA1	KAPPA	0.990	968	98.529	100
	TSS	0.990	605	100	99
	ROC	1.000	603	100	99
GLMRun3PA1	KAPPA	0.990	495	100	99.5
	TSS	0.995	495	100	99.5
	ROC	0.998	500	100	99.5
GAMRun3PA1	KAPPA	0.990	490	100	99.5
	TSS	0.995	490	100	99.5
	ROC	0.997	491.5	100	99.5
RFRun3PA1	KAPPA	0.990	414	100	99.5
	TSS	0.995	414	100	99.5
	ROC	1.000	414	100	99.5
GBMRun3PA1	KAPPA	0.990	500	100	99.5
	TSS	0.995	500	100	99.5
	ROC	1.000	498.5	100	99.5
GLMRun1PA2	KAPPA	0.971	495	98.529	99
	TSS	0.975	495	98.529	99
	ROC	0.988	500	98.529	99

Model ID	Evaluation Metric	Testing Data	Cutoff	Sensitivity	Specificity
GAMRun1PA2	KAPPA	0.980	949	98.529	98.5
	TSS	0.985	5	100	98.5
	ROC	0.997	10	100	98.5
RFRun1PA2	KAPPA	0.990	813	100	99.5
	TSS	0.995	813	100	99.5
	ROC	1.000	815	100	99.5
GBMRun1PA2	KAPPA	0.971	499	100	98.5
	TSS	0.985	499	100	98.5
	ROC	0.999	496	100	98.5
GLMRun2PA2	KAPPA	0.971	495	100	98.5
	TSS	0.985	495	100	98.5
	ROC	0.993	500	100	98.5
GAMRun2PA2	KAPPA	0.971	495	100	98.5
	TSS	0.985	495	100	98.5
	ROC	0.993	500	100	98.5
RFRun2PA2	KAPPA	0.971	374	100	98.5
	TSS	0.985	374	100	98.5
	ROC	0.997	375	100	98.5
GBMRun2PA2	KAPPA	0.971	498.5	100	98.5
	TSS	0.985	498.5	100	98.5
	ROC	0.994	498	100	98.5
GLMRun3PA2	KAPPA	0.990	495	100	99.5
	TSS	0.995	495	100	99.5
	ROC	0.998	500	100	99.5
GAMRun3PA2	KAPPA	0.980	495	98.529	99.5
	TSS	0.980	495	98.529	99.5
	ROC	0.990	500	98.529	99.5
RFRun3PA2	KAPPA	0.990	303	100	99.5
	TSS	0.995	303	100	99.5
	ROC	1.000	300	100	99.5
GBMRun3PA2	KAPPA	0.990	459	100	99.5
	TSS	0.995	459	100	99.5
	ROC	0.999	456.5	100	99.5
GLMRun1PA3	KAPPA	0.933	763	100	96.5
	TSS	0.965	763	100	96.5
	ROC	0.981	763	100	96.5
GAMRun1PA3	KAPPA	0.923	490	98.529	96.5
	TSS	0.950	490	98.529	96.5
	ROC	0.974	491	98.529	96.5
RFRun1PA3	KAPPA	0.952	449.5	100	97.5
	TSS	0.975	449.5	100	97.5
	ROC	0.998	452	100	97.5
GBMRun1PA3	KAPPA	0.961	914	100	98
	TSS	0.980	914	100	98

Model ID	Evaluation Metric	Testing Data	Cutoff	Sensitivity	Specificity
	ROC	0.996	914	100	98
GLMRun2PA3	KAPPA	0.971	889	100	98.5
	TSS	0.985	889	100	98.5
	ROC	0.991	891	100	98.5
GAMRun2PA3	KAPPA	0.971	520	100	98.5
	TSS	0.985	520	100	98.5
	ROC	0.993	524.5	100	98.5
RFRun2PA3	KAPPA	0.971	545	100	98.5
	TSS	0.985	545	100	98.5
	ROC	0.996	547	100	98.5
GBMRun2PA3	KAPPA	0.971	945	98.529	99
	TSS	0.980	253	100	98
	ROC	0.994	255	100	98
GLMRun3PA3	KAPPA	0.961	611	100	98
	TSS	0.980	611	100	98
	ROC	0.990	614.5	100	98
GAMRun3PA3	KAPPA	0.961	0.0	100	0
	TSS	0.980	0.0	100	0
	ROC	0.991	2.5	100	98
RFRun3PA3	KAPPA	0.961	677	98.529	98.5
	TSS	0.975	217	100	97.5
	ROC	0.997	219	100	97.5
GBMRun3PA3	KAPPA	0.961	604	100	98
	TSS	0.980	604	100	98
	ROC	0.993	605.5	100	98

LITERATURE CITED

Ahmadi-Nedushan, B., St-Hilaire, A., Bérubé, M., Robichaud, É., Thiémonge, N., & Bobée, B. (2006). A review of statistical methods for the evaluation of aquatic habitat suitability for instream flow assessment. *River Research and Applications*, *22*(5), 503–523.

Bailey, C. M., & Ware, S. (1990). Red Spruce Forests of Highland County , Virginia : Biogeographical Considerations. *Sourthern Appalachian Botanical Society*, *55*(4), 245–258.

Beane, N. R. (2010). *Using environmental and site-specific variables to model current and future distribution of red spruce (Picea rubens) forest habitat in West Virginia*. 178.

Beane, N. R., Rentch, J. S., & Schuler, T. M. (2013). *Using maximum entropy modeling to identify and prioritize red spruce forest habitat in West Virginia*. 16.

Bell, D. M., Bradford, J. B., & Lauenroth, W. K. (2014). Mountain landscapes offer few opportunities for high-elevation tree species migration. *Global Change Biology*, *20*(5), 1441–1451.

Bliss, M., & Vogelmann, H. W. (1982). Decline of Red Spruce in the Green Mountains of Vermont. *Torrey Botanical Society*, *109*(2), 162–168.

Blum, B. M. (1990). Red Spruce. In *Silvics of North America: Conifers* (pp. 250–259). Forest Service, United States Department of Agriculture.

Breiman, L. (2001). Random forests. *Machine Learning*, 45:5 -32.

Chen, X., & Leites, L. (2020). The importance of land-use legacies for modeling present-day species distributions. *Landscape Ecology*, *35*(12), 2759–2775.

Davis, V., Burger, J. A., Rathfon, R. A., & Zipper, C. E. (2017). Chapter 7: Selecting tree species for reforestation of Appalachian mined lands. In The Forestry Reclamation Approach: guide to successful reforestation of mined lands.

Dillard, L. O., Russell, K. R., & Ford, W. M. (2008). Site-level habitat models for the endemic, threatened Cheat Mountain salamander (Plethodon nettingi): The importance of geophysical and biotic attributes for predicting occurrence. *Biodiversity and Conservation*, *17*(6), 1475–1492.

Dumais, D., & Prévost, M. (2007). Management for red spruce conservation in Québec: The importance of some physiological and ecological characteristics - A review. *Forestry Chronicle*, *83*(3), 378–392.

Elith J., Ferrier S., Huettmann F., Leathwick J. (2005). The evaluation strip: A new and robust method for plotting predicted responses from species distribution models. Ecological Modelling. 186(3), 280 – 289.

Ford, W. M., Stephenson, S. L., Menzel, J. M., Black, D. R., & Edwards, J. W. (2004). Habitat characteristics of the endangered Virginia northern flying squirrel (Glaucomys sabrinus fuscus) in the central Appalachian Mountains. *American Midland Naturalist*, *152*(2), 430–438.

Gehrig-Fasel, J., Guisan, A., & Zimmermann, N. E. (2007). Tree line shifts in the Swiss Alps: Climate change or land abandonment? *Journal of Vegetation Science*, *18*(4), 571–582.

Goelz, J. C. G., Burk, T. E., & Zedaker, S. M. (1999). Long-term growth trends of red spruce and fraser fir at Mt. Rogers, Virginia and Mt. Mitchell, North Carolina. *Forest Ecology and Management*, *115*(1), 49–59.

Griscom, B., Griscom, H., & Deacon, S. (2011). Species-specific barriers to tree regeneration in high elevation habitats of West Virginia. *Restoration Ecology*, *19*(5), 660–670.

Guisan, A., Thuiller, W., & Zimmerman, N. E. (2017). *Habitat Suitability and Distribution Models With Applications in R*. Cambridge University Press.

Guisan, A., & Thuiller, W. (2005). Predicting species distribution: Offering more than simple habitat models. *Ecology Letters*, *8*(9), 993–1009.

Hernandez, P. A., Graham, C. H., Master, L. L., & Albert, D. L. (2006). The effect of sample size and species characteristics on performance of different species distribution modeling methods. *Ecography*, *29*(5), 773–785.

Horikawa, M., Tsuyama, I., Matsui, T., Kominami, Y., & Tanaka, N. (2009). Assessing the potential impacts of climate change on the alpine habitat suitability of Japanese stone pine (Pinus pumila). *Landscape Ecology*, *24*(1), 115–128.

Iverson, L. R., Prasad, A. M., Matthews, S. N., & Peters, M. (2008). Estimating potential habitat for 134 eastern US tree species under six climate scenarios. *Forest Ecology and Management*, *254*(3), 390–406.

Iverson, L., Prasad, A., Matthews, S., Peters, M., & Hoover, C. (2009). Potential changes in habitat suitability under climate change: Lessons learned from 15 years of species modelling. *XIII World Forestry Congress Buenos Aires. Argentina*, *October*, 18–23.

Johnson, A. H., Cook, E. R., & Siccama, T. G. (1988). Climate and red spruce growth and decline in the northern Appalachians. *Proceedings of the National Academy of Sciences*, *85*(15), 5369–5373.

Johnson, A. H., Shwartzman, T. N., Battles, J. J., Miller, R., Miller, E. K., Friedland, A. J., & Vann, D. R. (1994). Acid rain and soils of the Adirondacks. II. Evaluation of calcium and aluminum as causes of red spruce decline at Whiteface Mountain, New York. *Canadian Journal of Forest Research*, *24*(4), 654–662.

Kapos, V., Rhind, J., Edwards, M., Price, M. F., & Ravilious, C. (2000). *Developing a map of the world's mountain forests* (M. F. Price & N. Butt (eds.)). CABI Publishing.

Kaschner, K., Watson, R., & Trites, A. W. (2006). Mapping world-wide distributions of marine mammal species using a relative environmental suitability (RES) model . *Marine Ecology Progress Series*, *316*, 285–310.

Koo, K. A., Madden, M., & Patten, B. C. (2014). Projection of red spruce (Picea rubens Sargent) habitat suitability and distribution in the Southern Appalachian Mountains, USA. *Ecological Modelling*, *293*, 91–101.

Koo, K. A., Patten, B. C., & Creed, I. F. (2011). Picea rubens growth at high versus low elevations in the Great Smoky Mountains National Park: Evaluation by systems modeling. *Canadian Journal of Forest Research*, *41*(5), 945–962.

Landis, J. R. & Koch, G. G. (1977). The measurement of observer agreement for categorical data. *Biometrics*, *1*, 159-174.

Leblond, M., Dussault, C., & St-Laurent, M. H. (2014). Development and validation of an expert-based habitat suitability model to support boreal caribou conservation. *Biological Conservation*, *177*, 100–108.

Li, W., Kershaw, J. A., Costanza, K. K. L., & Taylor, A. R. (2020). Evaluating the potential of red spruce (Picea rubens Sarg.) to persist under climate change using historic provenance trials in eastern Canada. *Forest Ecology and Management*, *466*(February), 118139.

Liniger, H., & Weingartner, R. (2000). Mountain forests and their role in providing freshwater resources. In Mountain forests and their role in providing freshwater resources. 5, 370-380. CABI Publishing.

Mathias, J. M., & Thomas, R. B. (2018). Disentangling the effects of acidic air pollution, atmospheric CO2, and climate change on recent growth of red spruce trees in the Central Appalachian Mountains. *Global Change Biology*, *24*(9), 3938–3953.

McLaughlin S.B., Downing D.J., Blasing T.J., Cook E.R., A. H. S. (1987). An analysis of climate and competition as contributors to decline. *Environmental Sciences*, 487–501.

McManamay R.H., Resler L.M., Campbell J.B., McManamay R.A. (2011) Assessing the Impacts of Balsam Woolly Adelgid (Adelges piceae Ratz.) and Anthropogenic Disturbance on the Stand Structure and Mortality of Fraser Fir [Abies fraseri (Pursh) Poir.] in the Black Mountains, North Carolina. Castanea. 76(1), 1 – 19.

Murphy, L. S. (1917). *The Red Spruce: Its Growth and Management*. U.S. Department of Agriculture.

Normand, S., Randin, C., Ohlemüller, R., Bay, C., Høye, T. T., Kjær, E. D., Körner, C., Lischke, H., Maiorano, L., Paulsen, J., Pearman, P. B., Psomas, A., Treier, U. A., Zimmermann, N. E., & Svenning, J. C. (2013). A greener Greenland? Climatic potential and long-term constraints on future expansions of trees and shrubs. *Philosophical Transactions of the Royal Society B: Biological Sciences*, *368*(1624), 1–12.

Nowacki, G., Carr, R., & Van Dyck, M. (2010). the Current Status of Red Spruce in the Eastern United States : Distribution , Population Trends , and Environmental

Drivers. *Conference on the Ecology and Management of High-Elevation Forests in the Central and Southern Appalachian Mountains*, 140–162.

Nowacki, G., & Wendt, D. (2013). the Current Distribution , Predictive Modeling , and Restoration. *Proceedings from the Conference on the Ecology and Management of High-Elevation Forests in the Central and Southern Appalachian Mountains*, 163–178.

Odom, R. H., Ford, W. M., Edwards, J. W., Stihler, C. W., & Menzel, J. M. (2001). Developing a habitat model for the endangered Virginia northern flying squirrel (*Glaucomys sabrinus fuscus*) in the Allegheny Mountains of West Virginia. *Biological Conservation*, *99*(2), 245–252.

Pan, Y., Birdsey, R. A., Fang, J., Houghton, R., Kauppi, P. E., Kurz, W. A., Phillips, O. L., Shvidenko, A., Lewis, S. L., Canadell, J. G., Ciais, P., Jackson, R. B., Pacala, S. W., McGuire, A. D., Piao, S., Rautiainen, A., Sitch, S., & Hayes, D. (2011). A Large and Persistent Carbon Sink in the World's Forests. *Science*, *333*(6045), 988 LP – 993.

Parmesan, C., & Yohe, G. (2003). A globally coherent fingerprint of climate change impacts across natural systems. *Nature*, *421*(6918), 37–42.

Pielke, R. (1981). The distribution of spruce in west-central Virginia before lumbering. *Southern Appalachian Botanical Society*, *46*(3), 201–216.

Potter, K. M., Hargrove, W. W., & Koch, F. H. (2010). Proceedings from the Conference on the Ecology and Management of High-Elevation Forests in the Central and Southern Appalachian Mountains. *The Conference on the Ecology and Management of High-Elevation Forests in the Central and Southern Appalachian Mountains.*, 179–189.

Price, M. F., & Price, M. F. (2003). *Why mountain forests are important 1*. *79*(2), 1998–2001.

Rentch, J. S., Ford, W. M., Schuler, T. S., Palmer, J., & Diggins, C. A. (2016). Release of Suppressed Red Spruce Using Canopy Gap Creation - Ecological Restoration in the Central Appalachians. *Natural Areas Journal*, *36*(1), 29–37.

Rentch, J. S., Schuler, T. M., Ford, W. M., & Nowacki, G. J. (2007). Red Spruce Stsand Dynamics, Simulations, and Restoration Opportunities in the Central Appalachians. *Restoration Ecology*, *15*, 440–452.

Rentch, J. S., Schuler, T. M., Nowacki, G. J., Beane, N. R., & Ford, W. M. (2010). Canopy gap dynamics of second-growth red spruce-northern hardwood stands in West Virginia. *Forest Ecology and Management*, *260*(10), 1921–1929.

Ridgeway, G. (1999). The state of boosting. *Computing Science and Statistics*, *31*, 172–181.

Seymour, R. S. (1992). The red spruce-balsam fir forest of Maine: Evolution of silvicultural practice in response to stand development patterns and disturbances. In *The Ecology and Silviculture of Mixed-Species Forests*. Springer, Dordrecht.

Spaulding H.L., Rieske L.K. (2010). The aftermath of an invasion: Structure and composition of Central Appalachian hemlock forests following establishment of the hemlock woolly adelgid, *Adelges tsugae*. Biological Invasions. 12, 3153 - 3143

Sultana, S., Baumgartner, J. B., Dominiak, B. C., Royer, J. E., & Beaumont, L. J. (2017). Potential impacts of climate change on habitat suitability for the Queensland fruit fly. *Scientific Reports*, *7*(1), 1–10.

Swart N. C., Cole J. N., Kharin V. V., Lazare M., Scinocca J. F., Gillet N.P., Anstey J., Arora V., Christian J. R., Hanna S., Jiao Y. (2019). The Canadian earth system model version 5 (CanESM5. 0.3). *Geoscientific Model Development, 12*(11), 4823-4873.

Thomas-Van Gundy, M. A., & Sturtevant, B. R. (2014). Using Scenario modeling for red spruce restoration planning in West Virginia. *Journal of Forestry*, *112*(5), 457–466.

Thuiller, W. (2004). Patterns and uncertainties of species' range shift under climate change. *Global Change Biology*, *10*, 2020–2027.

Thuiller, W., Lavorel, S., Araújo, M. B., Sykes, M. T., & Prentice, I. C. (2005). Climate change threats to plant diversity in Europe. *Proceedings of the National Academy of Sciences of the United States of America*, *102*(23), 8245–8250.

Thuiller W., Lafourcade B., Engler R., & Araujo M.B. (2009). BIOMOD – a Platform for Ensemble Forecasting of Species Distributions. *Ecography, 32*, 369-373.

Walter, J. A., Neblett, J. C., Atkins, J. W., & Epstein, H. E. (2017). Regional- and watershed-scale analysis of red spruce habitat in the southeastern United States: implications for future restoration efforts. *Plant Ecology*, *218*(3), 305–316.

Williams-Tripp, M., D'Amico, F. J. N., Pagé, C., Bertrand, A., Némoz, M., & Brown, J. A. (2012). Modeling Rare Species Distribution at the Edge: The Case for the Vulnerable Endemic Pyrenean Desman in France.

Wisz, M. S., Hijmans, R. J., Li, J., Peterson, A. T., Graham, C. H., Guisan, A., Elith, J., Dudík, M., Ferrier, S., Huettmann, F., Leathwick, J. R., Lehmann, A., Lohmann, L., Loiselle, B. A., Manion, G., Moritz, C., Nakamura, M., Nakazawa, Y., Overton, J. M. C., … Zimmermann, N. E. (2008). Effects of sample size on the performance of species distribution models. *Diversity and Distributions*, *14*(5), 763–773.

Wisz, M. S., & Guisan, A. (2009). Do pseudo-absence selection strategies influence species distribution models and their predictions? An information-theoretic approach based on simulated data. *BMC Ecology, 9*, 1–13.

Wood, S. N. (2006). On confidence intervals for generalized additive models based on penalized regression splines. *Australian and New Zealand Journal of Statistics, 48*(4), 445–464.